Inflammatory Bowel Diseases

# Decellularized human gut as a natural 3D-platform for research in intestinal fibrosis

--Manuscript Draft--

| | |
|---|---|
| **Manuscript Number:** | IBD-D-19-00227R1 |
| **Article Type:** | Original Research Articles - Basic Science |
| **Section/Category:** | Therapy |
| **Keywords:** | Decellularization; human intestinal myofibroblast; 3D ECM scaffold in vitro model; tissue regeneration. |
| **Corresponding Author:** | Giuseppe Mazza, PhD<br>University College London Medical School<br>London, UNITED KINGDOM |
| **First Author:** | Paolo Giuffrida |
| **Order of Authors:** | Paolo Giuffrida |
| | Marco Curti |
| | Walid Al-Akkad |
| | Carin Biel |
| | Claire Crowley |
| | Luca Frenguelli |
| | Andrea Telese |
| | Andrew Hall |
| | Domenico Tamburrino |
| | Gabriele Spoletini |
| | Giuseppe Fusai |
| | Francesco Paolo Tinozzi |
| | Andrea Pietrabissa |
| | Gino Roberto Corazza |
| | Paolo De Coppi |
| | Massimo Pinzani |
| | Antonio Di Sabatino |
| | Krista Rombouts |
| | Giuseppe Mazza, PhD |
| **Manuscript Region of Origin:** | UNITED KINGDOM |
| **Abstract:** | Background: The current methodologies for the identification of therapeutic targets for inflammatory bowel disease (IBD) are limited to conventional two-dimensional (2D) cell cultures and animal models. The use of 3D decellularized human intestinal scaffolds obtained from surgically resected intestine and engineered with human intestinal cells may provide a major advancement in the development of innovative intestinal disease models. Aim of the present study was to design and validate a decellularization protocol for the production of acellular 3D extracellular matrix (ECM) scaffolds from human duodenum.<br>Methods: Scaffolds were characterized by verifying the preservation of the ECM protein composition and 3D architecture of the native intestine and were employed for tissue engineering with primary human intestinal myofibroblasts for up to 14 days.<br>Results: Engrafted cells showed the ability to grow and remodel the surrounding ECM. mRNA expression of key genes involved in ECM turnover was significantly different |

| | |
|---|---|
| | when comparing primary human intestinal myofibroblasts cultured in 3D scaffolds with these cultured in standard 2D cultures on plastic dishes. Moreover, incubation with key pro-fibrogenic growth factors such as TGFβ1 and PDGF-BB resulted in markedly different effects in standard 2D versus 3D cultures, further emphasizing the importance of using 3D cell cultures.<br>Conclusions: These results confirm the feasibility of 3D culture of human intestinal myofibroblasts in intestinal ECM scaffolds as an innovative platform for disease modelling, biomarker discovery and drug testing in intestinal fibrosis. |

# Decellularized human gut as a natural 3D-platform for research in intestinal fibrosis

Running Head: Bioengineering of human gut ECM 3D scaffolds

Paolo Giuffrida[1,2*], Marco Curti[1,2*], Walid Al-Akkad,[1] Carin Biel[1], Claire Crowley[3], Luca Frenguelli[1], Andrea Telese[1], Andrew Hall[1], Domenico Tamburrino[4], Gabriele Spoletini[4], Giuseppe Fusai[4], Francesco Paolo Tinozzi[5], Andrea Pietrabissa[5], Gino Roberto Corazza[2], Paolo De Coppi[3,6], Massimo Pinzani[1], Antonio Di Sabatino[1,2], Krista Rombouts[1&], Giuseppe Mazza[1&#]

[1]Regenerative Medicine & Fibrosis Group, Institute for Liver & Digestive Health, University College London, Royal Free Hospital, London, UK

[2]First Department of Internal Medicine, San Matteo Hospital Foundation, University of Pavia, Pavia, Italy.

[3]Stem Cells and Regenerative Medicine Section, Developmental Biology and Cancer Programme, UCL Institute for Child Health, Great Ormond Street Hospital. University College London, London UK.

[4]Division of Surgery, University College London, Royal Free, London, UK.

[5]Department of Surgery, General Surgery II, San Matteo Hospital Foundation, University of Pavia, Pavia, Italy.

[6]Specialist Neonatal and Paediatric Surgery at Great Ormond Street Hospital, London, UK

* PG and MC contributed equally to this manuscript and should be considered joint first authors.

& KR and GM contributed equally to this manuscript and should be considered joint senior authors

**Word count**: 3,871

**Abbreviations**: ECM, extracellular matrix; EVG, elastin Van Gieson; H&E, haematoxylin and eosin; IDA, industrial denatured alcohol; MMP, matrix metalloproteinase; PDGF, platelet-derived growth factor; R-a, ring-agitation; SEM, scanning electron microscopy; SR, picro-sirius red; TGF, transforming growth factor; 2D, two-dimensional; 3D, three-dimensional.

[#]**Address for correspondence**: Dr Giuseppe Mazza, Institute for Liver and Digestive Health, UCL Royal Free Campus, Rowland Hill Street, NW3 2PF, London, UK. E-mail: giuseppe.mazza.12@ucl.ac.uk

**Acknowledgements**

This work was supported by the National Institute for Health Research (NIHR), University College London Biomedical Research Centre III (to GM) and the Royal Free Charity (to MP). PDC is supported by NIHR, CC and PDC are supported by the OAK Foundation.

**Author Disclosure Statement**

No competing financial interests exist.

**Summary**

We successfully developed a novel and reproducible protocol designed to "decellularize-recellularize" acellular 3D extracellular matrix (ECM) scaffolds from human intestine. 3D cultures of intestinal myofibroblasts in ECM scaffolds represent a key alterative to 2D cultures on plastic and animal models.

## ABSTRACT

**Background:** The current methodologies for the identification of therapeutic targets for inflammatory bowel disease (IBD) are limited to conventional two-dimensional (2D) cell cultures and animal models. The use of 3D decellularized human intestinal scaffolds obtained from surgically resected intestine and engineered with human intestinal cells may provide a major advancement in the development of innovative intestinal disease models. Aim of the present study was to design and validate a decellularization protocol for the production of acellular 3D extracellular matrix (ECM) scaffolds from human duodenum.

**Methods:** Scaffolds were characterized by verifying the preservation of the ECM protein composition and 3D architecture of the native intestine and were employed for tissue engineering with primary human intestinal myofibroblasts for up to 14 days.

**Results:** Engrafted cells showed the ability to grow and remodel the surrounding ECM. mRNA expression of key genes involved in ECM turnover was significantly different when comparing primary human intestinal myofibroblasts cultured in 3D scaffolds with these cultured in standard 2D cultures on plastic dishes. Moreover, incubation with key pro-fibrogenic growth factors such as TGFβ1 and PDGF-BB resulted in markedly different effects in standard 2D versus 3D cultures, further emphasizing the importance of using 3D cell cultures.

**Conclusions:** These results confirm the feasibility of 3D culture of human intestinal myofibroblasts in intestinal ECM scaffolds as an innovative platform for disease modelling, biomarker discovery and drug testing in intestinal fibrosis.


**Keywords**: decellularization; human intestinal myofibroblast; 3D ECM scaffold *in vitro* model; tissue regeneration.

## INTRODUCTION

Intestinal fibrosis represents a common consequence of chronic inflammation in inflammatory bowel disease (IBD) and is characterized by the accumulation of fibrillar extracellular matrix (ECM) by activated myofibroblasts.[1] In particular, intestinal fibrosis affects around 40% of patients with Crohn's disease and 5% of patients with ulcerative colitis.[2,3] The lack of an effective medical anti-fibrotic therapy and reliable non-invasive biomarkers still represents an important unmet clinical need in IBD.[2,3]

The traditional platforms used for disease modelling and drug screening in IBD are two-dimensional (2D) cell monolayers cultured on plastic surfaces, animal models and human organ cultures. However, cells in monolayer cultures tend to de-differentiate because of the high stiffness of the artificial substrate. Thus cellular functions may be affected by the lack of signals from other stromal cells and ECM proteins organized within a tissue-specific 3D architecture.[4] Animal models overcome some of the 2D model limitations by providing physiological features inherent to the gastrointestinal microenvironment, 3D architecture and multicellular complexity. However, most animal models do not fully recapitulate human IBD pathophysiology,[5] are not cost-effective[6] and are burdened by ethical issues.[7] Human organ cultures provide intercellular and cell-ECM networks in a naturally 3D endogenous environment, but they are restricted by low amounts of samples -in particular for the deepest intestinal layers- and by a reduced tissue viability due to poor delivery of oxygen and nutrients, mainly for prolonged cultures.[8] Therefore, due to the high prevalence of gastrointestinal disorders, there is a pressing demand to establish *in vitro* models of human IBD and to develop drug-screening platforms that more accurately recapitulate the complex physiology of the human fibrotic intestine.[9] Tissue engineering has provided new 3D platform technologies, such as organoids, spheroids and scaffolds for the *in vitro* study of pathophysiological mechanisms underlying gastrointestinal disorders. Organoids, which are derived from tissue obtained from biopsies or surgical sections, are 3D cultures which can contain epithelium, and/or pluripotent stem cells, are characterized by high costs of maintenance, lack of proper stromal and ECM components

in addition to high variability between different laboratories.[10] The use of spheroids allows the growth of human intestinal epithelial cells isolated from mucosal biopsies[11] with a tendency to preserve the region-specific cell differentiation.[12] However, one of the key challenge is the reproducibility of this tool due to size variability.[13] Synthetic intestinal scaffolds can be manufactured with a wide range of materials.[14] However, their main limitation is the absence of the physiological tissue-specific ECM complexity with consequent suboptimal biocompatibility both *in vitro* and *in vivo*.[4,15] Accordingly, biological ECM scaffolds have been successfully obtained by decellularization of human and murine organs, including liver.[16-18] In previous studies we have demonstrated the feasibility of the "decellularization and recellularization" technology of human liver 3D scaffolds which constitutes a valuable platform for liver bioengineering through the repopulation of human liver ECM scaffolds with parenchymal and non-parenchymal liver cells.[16,19] The project herein presented was aimed at the development of a well-defined 3D *in vitro* model based on acellular human gut ECM scaffold engineered with primary human intestinal myofibroblasts and at evaluating the suitability of this construct for disease modelling and target discovery in the high demand area of intestinal fibrosis.

## MATERIALS AND METHODS

**Sources of reagents.** Unless otherwise specified, all reagents were purchased from Sigma.

**Source of human duodena and tissue preparation.** Healthy human duodena (n=5), explanted by Whipple procedure, were obtained under local ethics from the UCL Royal Free BioBank Ethical Review Committee (NRES Rec Reference: 11/WA/0077). Informed consent was given by each patient taking part in the study. Intestines were washed with 1% PBS solution to clear from blood and luminal contents, dried and frozen at -80 °C for at least 24h.

**Decellularization protocol.** Prior to decellularization, intestines were thawed in a 37°C water bath for 1h, and maintained during the decellularization protocol as long duodenal segments of 9 cm. Once decellularized segments were dissected into 3 cm long rings and later into 1 x 0.5 cm squares The decellularization protocol based on ring agitation (R-a) is shown in Table 1 and Fig. 1A. The resultant tissues were further characterized by employing histological, immunohistochemical studies as well as DNA and collagen quantification.

**Histology.** After the decellularization procedure, samples were fixed for at least 24h in 10% neutral buffered formalin solution (pH 7.4) at room temperature then embedded in paraffin and sectioned at 4 μm. Prior to staining, sections were dewaxed in xylene and rehydrated using a series of graded industrial denatured alcohol (IDA) and water. Tissue sections were stained with Harris's Haematoxylin and Eosin (H&E) (Leica, Germany), Picro-Sirius Red (SR) (Hopkin & Williams) (BDH Chemicals Ltd, Cellpath Ltd) and Miller's Elastic stain with a Picro-Sirius red counter stain (Elastin Van Gieson, EVG) (VWR, Leica, Raymond A Lamb) as previously described.[16]

**Immunohistochemistry.** Sections were incubated in 0.5% Trypsin (MP Biomedical)/0.5% Chymotrypsin (Sigma)/1% Calcium Chloride (BDH) in Tris buffered saline pH 7.6 (TBS) for 30

minutes at 37 °C as previously described.[16]. Slides were then soaked in TBS with 0.04% Tween-20 (Sigma) for 5 minutes, blocked in peroxidase blocking solution (Novocastra) for 5 minutes, washed in TBS for 5 minutes and then incubated for 1h with one of the following primary antibodies: rabbit polyclonal to collagen I (ab34710, 1:200, Abcam), rabbit polyclonal to collagen III (ab7778, 1:500, Abcam), mouse monoclonal to collagen IV (M0785, 1:25, Dako), mouse monoclonal to fibronectin (MAB1937, 1:100, Millipore) and mouse monoclonal to laminin α5-chain (MAB1924, 1:200, Millipore). The slides were then placed for 25 minutes in NovolinkTM post primary (Novocastra), 25 minutes in NovolinkTM polymer solution (Novocastra) and developed with NovolinkTM 3,3′ di-amino-benzidine (Novocastra) with a 5 minutes wash in TBS with 0.04% Tween-20 between each step. Slides were counterstained with Mayer's Haematoxylin (Sigma) for 3 minutes. All sections were dehydrated in graded IDA and xylene and were mounted with DPX (Leica biosystems); cover slipped and observed using a Zeiss Axioskop 40. Images were captured with an Axiocam IcC5 using Zeiss Axiovision (verison 4.8.2). All images were analyzed and enhanced using Fiji v1.49d (ImageJ Jenkins server).

**DNA quantification.** To assess total DNA content within native tissue and acellular matrices, the DNeasy Blood and Tissue kit was used according to the manufacturer's manual (Qiagen) and as described previously.[16,20] Briefly, specimens were digested with Proteinase K overnight. DNA samples were purified using buffers provided by the company and measured spectrophotometrically (Nanodrop, Thermo Scientific, US). Optical densities at 260 nm and 280 nm were used to estimate the purity and yield of nucleic acids.

**Collagen quantification.** The collagen content of native tissue and decellularized tissue was quantified as described previously[16] using the total collagen assay kit according to the manufacturer's manual (QuickZyme Biosciences, The Netherlands). Briefly, samples were hydrolyzed in 6M HCl at 95°C for 20h, the hydrolysates were mixed with a chromogen solution

staining the hydroxyproline residues and color was developed at 60°C for 1h. The absorbance for each sample was determined at 555 nm using a FLUOstar Omega microplate reader (BMG labtech, Germany) and the collagen quantity was calculated by employing a standard curve of pure collagen hydrolysates.

**Scanning Electron Microscopy (SEM).** Samples were fixed in 2.5% glutaraldehyde in 0.1 M phosphate buffer and left for 24h at 4°C, as previously described.[16] Briefly, following washing with 0.1 M phosphate buffer, samples were cut into segments of approximately 1 cm length and cryoprotected in 25% sucrose, 10% glycerol in 0.05 M PBS (pH 7.4) for 2h, then fast frozen in Nitrogen slush and fractured at approximately − 160°C. Next, samples were placed back into the cryoprotectant at room temperature and allowed to thaw. After washing in 0.1 M phosphate buffer (pH 7.4), the material was fixed in 1% $OsO_4$ / 0.1 M phosphate buffer (pH 7.3) at 3°C for 1½h and washed again in 0.1 M phosphate buffer (pH 7.4). After rinsing with distilled water, specimens were dehydrated in a graded ethanol-water series to 100% ethanol; critical point dried using $CO_2$ and finally mounted on aluminium stubs using sticky carbon taps. The fractured material was mounted to present fractured surfaces across the parenchyma to the beam and coated with a thin layer of Au/Pd (approximately 2 nm thick) using a Gatan ion beam coater. Images were recorded with a 7401 FEG scanning electron microscope (Jeol, USA).

**Sterilization of decellularized tissue.** Prior to in vitro cell seeding, intestinal cubes were sterilized by immersion in 0.1%PAA-4%EtOH for 45 minutes, followed by a washing step in sterile 1X PBS for 15 minutes. During both steps intestinal cubes were agitated using the Orbit M60 Digital Microtube Shaker at 900 rpm.

**Human intestinal myofibroblast isolation and culture.** Cells were isolated as previously described.[21] Briefly, the epithelial layer was removed by 1 mM EDTA for two 30 minutes periods at

37°C. After EDTA treatment, intestinal mucosal samples were denuded of epithelial cells, and were subsequently cultured at 37°C in a humidified $CO_2$ incubator in Dulbecco's modified Eagle's medium (DMEM) supplemented with 20% fetal calf serum, 100 U/ml penicillin, 100 mg/ml streptomycin, 50 mg/ml gentamycin and 2.5 mg/ml amphotericin. During culture, numerous cells appeared both in suspension and adhered to the culture dish. The cells in suspension were removed every 24–72 h, and the denuded mucosal tissue was maintained in culture for up to 6 weeks. Established colonies of myofibroblasts were seeded into 25 $cm^2$ culture flasks and cultured in DMEM supplemented with 20% FCS and antibiotics. At confluence, the cells were passaged using trypsin-EDTA in a 1:2 to 1:3 split ratio. Cells were grown up to passage 7 – 10 before the final concentration was reached to perform experiments.

**Repopulation and culture of engineered human intestine.** Sterilized human gut scaffolds were kept overnight in complete medium [day -1]. Myofibroblasts were trypsinized and then re-suspended at a final concentration of 25,000 cells/µl. Scaffolds were reseeded with 20 µl of cell-containing medium (0.5 million cells/scaffold) by using the drop-on technique, as previously described.[16] Seeded scaffolds were kept for 2h in a humidified incubator at 37°C with 5% $CO_2$ allowing cell attachment followed by the addition of the complete culture medium [day 0]. The culture medium was changed at day 1 and afterwards every 3 days. At days 7 and 14 following seeding, the scaffolds were placed in 10% formalin and assessed by histology analysis.

**2D culture and 3D culture long-term treatment.** In order to compare myofibroblast cell behavior both 2D and 3D experiments were performed in parallel. At day 0, myofibroblasts (150,000 per well) were plated on a 6 well cell culture dish (Greiner Bio-one) or reseeded in intestinal scaffolds (0.5 million cells/scaffold). Long term treatment with platelet-derived growth factor (PDGF)-BB (10 ng/ml, PeproTech) or transforming growth factor (TGF)-β1 (10 ng/ml, R&D systems) was

started at day -1 up to day 12. Culture media plus stimuli was refreshed every 3 days. At day 12, scaffolds were snap frozen and stored at -80°C until RNA extraction.

**RNA extraction and quantitative real-time PCR (qPCR).** RNA was isolated from myofibroblasts cultured in scaffolds by using RNeasy® Plus Micro Kit (Qiagen) according to the manufactures' protocol. First the scaffolds were disrupted and homogenized by shaking for 5 min at 50Hz (Qiagen TissueLyser LT) with a 5 mm and a 7 mm stainless steel beats (Qiagen) in 350 µl Buffer RLT plus. RNA concentration and purity were measured with Nanodrop spectrophotometer (Thermo Scientific). RNA was isolated from the myofibroblasts cultured in 2D by using RNeasy® Mini Kit according to the manufactures' protocol. Complementary DNA (cDNA) was synthesized using the following reaction mix: MultiScribe reverse transcriptase, random primers, dNTP mix and RNase inhibitor (Applied Biosystems) and reverse transcription was performed with a Q Cycler II (Quanta Biotech). qPCR was performed by using Taqman gene assays (Applied Biosystems) for the following genes: GAPDH (Hs02758991_g1), ACTA2 (Hs00426835_g1), COL1A1 (Hs00164004_m1), TGFβ1 (Hs00998133_m1) and matrix metalloproteinase MMP-3 (Hs00968305_m1). The comparative Ct method was used to quantify relative gene expression, using Glyceraldehyde 3-phosphate dehydrogenase (GADPH) as internal control as previously described.[20,22]

**Statistical analysis.** Data were analyzed with the GraphPad Prism statistical PC program (GraphPad Software, San Diego, CA) using Anova or Student's t-test. Results were expressed as mean ± SEM or standard deviation (SD). Two-tailed p values less than 0.05 were considered statistically significant.

## RESULTS

**Decellularization of human duodenum.** Decellularization of the duodenum was completed within one week by employing the R-a protocol (Table 1). While progressing through the decellularization process, tissue rings became increasingly translucent (Fig. 1B). The R-a protocol is characterized by applying a combination of four different cell-damaging factors: (*i*) freezing/thawing, (*ii*) mechanical agitation by employing shaker, (*iii*) osmotic stress, i.e. distilled water and PBS, to allow cell lysis, and (*iv*) the detergent sodium deoxycholate to remove debris (Table 1). Histological assessment by H&E and SR staining showed no evidence of nuclear or cellular material in the decellularized 3D duodenum scaffolds (Fig. 1C). Moreover, the overall gut architecture appeared fully preserved as shown by SR staining for collagens and EVG staining for elastin (Fig. 1C). The efficacy of the R-a protocol was confirmed by the absence of quantifiable DNA material (Fig. 1D) as the DNA quantification demonstrated a significant DNA reduction in decellularized gut (mean 42.6 ± 11.6 ng/mg) in comparison to native gut (mean 846.4 ± 149.9 ng/mg) ($p<0.01$). Furthermore, no significant difference in collagen content was observed between decellularized gut (mean 44.3 ± 11.4 ng/mg) and native gut tissue (mean 57.6 ± 15.8 ng/mg) (Fig. 1E).

**Duodenal tissue scaffold characterization.** To assess the preservation of ECM components, the ECM expression and distribution of different ECM components were evaluated by immunohistochemistry (Fig. 2A-J). Five key structural ECM proteins, i.e. collagen I (Fig. 2B), collagen III (Fig. 2D), collagen IV (Fig. 2F), fibronectin (Fig. 2H) and laminin (Fig. 2J) were fully preserved following decellularization in comparison to native duodenal tissue (Fig. 2A,C,E,G,I). Furthermore, the distribution of each ECM protein within the duodenal scaffoldconfirmed the complete preservation of the architecture of the native duodenal tissue.

**Ultrastructural characterization of decellularized human duodenum.** SEM was performed to further investigate the effects of decellularization on the 3D-architecture and microstructure of the ECM (Fig. 3A-F). At low magnification, the 3D architecture of duodenal scaffolds (Fig. 3B) appeared to be preserved in comparison to the architecture of the native tissue (Fig. 3A). At intermediate and high magnification, in particular, the 3D-microstructure of villus/crypt ratio was demonstrated (Fig. 3D,F) and comparable to that of the native duodenal tissue (Fig. 3C,E).

**Bioengineering of human duodenal scaffolds with primary human intestinal myofibroblasts.** In order to evaluate the *in vitro* biocompatibility, human duodenal ECM scaffolds were reseeded with primary human intestinal myofibroblasts (Fig. 4A). The repopulated scaffolds were evaluated after 7 days up to 14 days of culture. H&E staining showed a progressive engraftment of primary human intestinal myofibroblasts into the scaffold over 14 days (Fig. 4B).

**Primary human intestinal myofibroblasts bioengineered in human duodenal 3D scaffolds display a different gene expression compared to standard 2D culture conditions.** Gene expression in primary human intestinal myofibroblasts was evaluated by culturing cells in standard 2D culture conditions and 3D intestinal scaffolds (Fig. 4C). Gene expression was evaluated by performing qPCR for the following markers ACTA2, COL1A1, TGF-β1, and MMP-3 typical of tissue wound healing/fibrogenesis. As illustrated in Figure 4C, significant differences in gene expression were detected comparing 2D versus 3D cultures. Specifically, ACTA2 and COL1A1 mRNA expression was more than 5 times higher in myofibroblasts cultured in 2D compared with fibroblasts cultured in 3D intestinal scaffolds (***$p<0.005$, 2D vs 3D). The expression of TGF-β1 was four times higher in fibroblasts cultured on intestinal scaffolds compared to myofibroblasts cultured in standard 2D culture conditions (**$p<0.01$, 2D vs 3D). MMP-3 expression was two times higher in the myofibroblasts cultured engrafting 3D intestinal scaffolds compared to myofibroblasts cultured in 2D culture (*** $p<0.005$, 2D vs 3D).

**Long term treatment with TGF-β1 or PDGF-BB.** In order to mimic a microenvironment closer to that of chronic intestinal disease, the bioengineered constructs were subjected to treatment for up to 12 days with TGFβ1 or PDGF-BB followed by histological analysis and assessment of gene expression and compared to standard 2D cultures. Cells repopulated in 3D scaffolds showed a stronger engraftment and intra-scaffold spreading with long-term PDGF-BB treatment (Fig. 5A) in comparison to control condition. TGF-β1 treatment induced a significant up-regulation of ACTA2 (*** $p<0.005$ vs control) only in 3D cultured myofibroblasts when compared to control (Fig. 6B). Cells cultured in 2D as well as 3D and long-term treated with PDGF-BB did not show any significant difference in ACTA2 mRNA expression (Fig. 5B). COL1A1 mRNA expression was significantly up-regulated upon TGF-β1 treatment in both 2D and 3D cultured fibroblasts in comparison to non-treated control cells (*** $p<0.005$ and ** $p<0.01$, respectively) (Fig. 5C). TGF-β1 expression did not significantly differ upon long-term treatment with TGF-β1 or PDGF-BB in standard 2D conditions, but was significantly up-regulated upon exogenous TGF-β1 treatment in 3D compared to the non-treated, control 3D culture (*** $p<0.005$) and 2D versus 3D treated cells, respectively (*** $p<0.005$ respectively) (Fig. 5D). MMP-3 mRNA expression in 2D cultured myofibroblasts treated with TGF-β1 was significantly decreased compared to non-treated control cells in 2D cultured (Fig, 5D, * $p<0.05$ control vs TGFβ1 treated in 2D). In 3D cultured TGFβ1-treated myofibroblasts, MMP-3 expression was significantly up-regulated in comparison to 2D culture treated cells (Fig. 5E, ** $p<0.01$ TGFβ1 treatment 2D vs 3D). Long-term treatment with PDGF-BB did not affect MMP-3 mRNA expression (Fig.5E).

## DISCUSSION

We report the successful development of a novel and reproducible methodology for the decellularization of human duodenum leading to the production of human intestinal 3D ECM scaffolds. This achievement represents an important basis for tissue engineering of the gut with the aim to develop research platforms for disease modelling, drug target and biomarker discovery in addition to drug efficacy testing in human intestinal fibrosis.

Decellularization of the gut of several animals, including rat and pig, had been previously reported with data demonstrating the conservation of key properties of connective tissue and vasculature.[23,24] Furthermore, the decellularization of human intestine had been already reported for regenerative medicine applications.[25] Differently, our primary aim was to decellularize human duodenal tissue and then proceed to the recellularization of the 3D scaffolds using human primary intestinal myofibroblasts to develop 3D models for the study of intestinal fibrosis. This latter development is highly awaited to overcome the experimental limitations of the currently available platforms, including standard 2D culture models, animal models, organoids, spheroids and synthetic scaffolds.

An important feature of the proposed decellularization procedure is the possibility of obtaining 3D intestinal ECM scaffolds from specimens obtained by routine surgical resections thus allowing a more widespread application in hospitals and academic centres. This natural 3D-platform represents a simple method based on four different cell-damaging factors, freezing/thawing, mechanical agitation, osmotic stress and the detergent sodium deoxycholate. Hundreds of 3D ECM scaffolds, 1 x 0.5 $cm^2$, are obtained from a gut ring and could be used for several experiments. However, the main limitation of this method is the training on decellularization-recellularization technique which might constitute a gap for other research groups. Another challenge might be difficulty in obtaining significantly long gut rings for research groups with no access to surgical specimens from Whipple procedures.

The use of an ECM platform in which biochemical and biomechanical ECM features are maintained is crucial for the development of tissue bioengineering aimed at regenerative and modelling

purposes. Accordingly, the current trend is to employ different ECM substrates in 3D configuration to improve the physiological microenvironment to study human cell behavior.[19] For example, recently published work has focused on a 3D organotypic model of human intestinal mucosa by using a bioreactor and collagen gel.[26] The results of the present study provides, for the first time, evidence of an efficient decellularization-recellularization of human 3D intestinal scaffolds which are characterized by the preservation of the key features of human intestinal ECM modulating fundamental cellular functions, such as differentiation, induction and maintenance of phenotype.**Error! Reference source not found.** In particular, the decellularization protocol showed the preservation of both collagen and elastin distribution. In terms of topographic distribution, the retention of the five key ECM proteins, namely collagen I, III and IV, fibronectin and laminin was observed by immunohistochemistry in the lamina propria, along the *muscularis mucosae* and around the submucosal blood vessels without significant differences with their distribution in the native tissue. In addition, SEM demonstrated that the 3D-architecture of mucosal ECM, in particular the villus/crypt ratio, was preserved. A key effort of this study was to evaluate in *vitro* biocompatibility of the scaffold when repopulated by organ-specific cells such as human primary intestinal myofibroblasts.[16,21,**Error! Reference source not found.**] Intestinal myofibroblasts demonstrated an effective engraftment in their typical anatomical location. In particular, they were able to engraft not only into the lamina propria, where the cells originally were isolated, but also into the submucosa and in the muscle layer. Moreover, the expression profile of phenotype-specific markers for primary human intestinal myofibroblasts indicated that the engrafted cells maintained higher cellular differentiation features as well as a less activated phenotype following prolonged culture in 3D scaffolds when compared to the same cell preparation grown in standard 2D-plastic conditions. Indeed, the mRNA expression of key pro-fibrogenic and ECM remodelling genes (ACTA2, COL1A1, TGFβ1 and MMP-3) showed a remarkable difference between 3D scaffold cultures and 2D standard culture conditions, thus confirming that the phenotype of primary cells can be dramatically affected by *in vitro* culture employing either artificial and non-physiological high

stiffness substrates.[20,Error! Reference source not found.] Along these lines, and similarly to what observed comparing cultures of human hepatic stellate cells in human liver 3D ECM scaffolds versus cultures of the same cells on plastic dishes,[20] it is evident that the upregulation of key pro-fibrogenic genes such as ACTA2 and COL1A1 is largely artificial and dependent on the high stiffness of the substrate rather than a physiological or pathophysiological response to growth factors such as TGF-β1.[30] The parallel higher TGF-β1 and MMP-3 gene expression observed in the 3D scaffolds compared to the 2D cultures further highlights and complete the divergence between the two types of culture platforms. In addition, the differences in baseline gene expression observed in different culture conditions are likely to condition the changes in gene expression following stimulation with TGF-β1. To further investigate the use of tissue-specific human ECM scaffolds for fibrostenotic IBD, we treated intestinal myofibroblasts cultured in 3D duodenal scaffolds and in 2D standard conditions with key pro-fibrogenic growth factors such as TGF-β1 and PDGF-BB.[31] Stimulation with both pro-fibrogenic mediators resulted in different effects on the expression of target mRNAs when comparing myofibroblasts cultured in 3D or 2D cultures. Again, these results emphasize the specific interaction between cells and the microenvironment, i.e. 2D versus 3D, and the effect of pro-fibrotic mediators. It is very plausible that the response to both TGF-β1 and PDGF-BB observed in fibroblasts cultured in 3D scaffolds is closer to the cellular *in vivo* response and also by taking into account the absence of specific integrin/cytoskeletal interactions in 2D which is necessary for a correct growth factor intracellular signalling.[32,33] Interestingly, TGF-β1 mRNA expression, already induced in 3D cultures in comparison to 2D cultures, is further up-regulated in 3D scaffolds by prolonged treatment of the cells with exogenous TGF-β1. Similar results were obtained for MMP-3 mRNA expression when cultured in 3D scaffolds compared to 2D cultures on plastic. This confirms that MMP-3 mRNA and protein expression are artificially down-regulated in myofibroblasts grown on rigid high stiffness 2D plastic substrata,[21] whereas this study demonstrates that MMP-3 gene expression can be further up-regulated by exogenous TGF-β1 stimulation in human 3D scaffolds cultures. Overall, these data highlight remarkable differences in cell biology

when cells are cultured in their own native 3D ECM scaffold and when compared with standard 2D culture conditions. Therefore, the novel *in vitro* 3D model described in the present study further adds accuracy and validity to the search for molecular targets of intestinal fibrosis. Similarly to co-culture of distinct cell types in other 3D scaffolds,[34] our 3D-platform could also have potential implications in investigating interactions between myofibroblasts and other intestinal cell types, such as epithelial cells and immune cells, in sequential, which might clarify the complexity of disease modelling and screen drugs in IBD more-in-depth. However, this lies outside of the aim of the present study.

In conclusion, the present study describes the development of a novel effective protocol for generating 3D tissue-specific ECM scaffolds to improve the knowledge on the pathogenesis of intestinal fibrosis including fibrostenotic IBD, to predict drug efficacy or toxicity, to discover biomarkers, and to reduce developmental costs of current models, i.e. 2D cultures and animal models.

**Contributors**

PG, WAA, PDC, MP, ADS, KR and GM designed the study. PG, MC, WAA, CB, CC, LF, AT and AH collected data. WAA, MP, ADS, DT, GS, GF, FPT, AP and GM provided material. All authors analyzed and interpreted the data. PG, MC and CB did the statistical analyses. PG, MC, CB, GRC, MP, ADS, KR, and GM wrote the manuscript. All authors approved the final report.

**References**


1. Lenti MV, Di Sabatino A. Intestinal fibrosis. *Mol Aspects Med*. 2019;65:100-109.
2. Rieder F, Bettenworth D, Ma C, et al. An expert consensus to standardise definitions, diagnosis and treatment targets for anti-fibrotic stricture therapies in Crohn's disease. *Aliment Pharmacol Ther*. 2018;48:347-357.
3. Giuffrida P, Pinzani M, Corazza GR, et al. Biomarkers of intestinal fibrosis - one step towards clinical trials for stricturing inflammatory bowel disease. *United European Gastroenterol J*. 2016;4:523-530.
4. Pereira JF, Awatade NT, Loureiro CA, et al. The third dimension: new developments in cell culture models for colorectal research. *Cell Mol Life Sci*. 2016;73:3971-3989.
5. Macdonald TT. Inside the microbial and immune labyrinth: totally gutted. *Nat Med*. 2010;16:1194-1195.
6. Huh D, Matthews BD, Mammoto A, et al. Reconstituting organ-level lung functions on a chip. *Science*. 2010;328:1662-1668.
7. Elliott NT, Yuan F. A review of three-dimensional in vitro tissue models for drug discovery and transport studies. *J Pharm Sci*. 2011;100:59-74.
8. Al-Lamki RS, Bradley JR, Pober JS. Human Organ Culture: Updating the Approach to Bridge the Gap from In Vitro to In Vivo in Inflammation, Cancer, and Stem Cell Biology. *Front Med (Lausanne)*. 2017;4:148.
9. Benam KH, Dauth S, Hassell B, et al. Engineered in vitro disease models. *Annu Rev Pathol*. 2015;10:195-262.
10. Dedhia PH, Bertaux-Skeirik N, Zavros Y, et al. Organoid Models of Human Gastrointestinal Development and Disease. *Gastroenterology*. 2016;150:1098-1112.
11. VanDussen KL, Marinshaw JM, Shaikh N, et al. Development of an enhanced human gastrointestinal epithelial culture system to facilitate patient-based assays. *Gut*. 2015;64:911-920.
12. Ray K. Intestinal tract. Patient-derived intestinal spheroids--culturing the gut. *Nat Rev Gastroenterol Hepatol*. 2014;11:516.
13. Fennema E, Rivron N, Rouwkema J, et al. Spheroid culture as a tool for creating 3D complex tissues. *Trends Biotechnol*. 2013;31:108-115.
14. Costello CM, Hongpeng J, Shaffiey S, et al. Synthetic small intestinal scaffolds for improved studies of intestinal differentiation. *Biotechnol Bioeng*. 2014;111:1222-1232.

15. Chan BP, Leong KW. Scaffolding in tissue engineering: general approaches and tissue-specific considerations. *Eur Spine J*. 2008;17 Suppl 4:467-79.

16. Mazza G, Rombouts K, Rennie Hall A, et al. Decellularized human liver as a natural 3D-scaffold for liver bioengineering and transplantation. *Sci Rep*. 2015;5:13079.

17. Mazza G, Simons JP, Al-Shawi R, et al. Amyloid persistence in decellularized liver: biochemical and histopathological characterization. *Amyloid*. 2016;23:1-7.

18. Uygun BE, Soto-Gutierrez A, Yagi H, et al. Organ reengineering through development of a transplantable recellularized liver graft using decellularized liver matrix. *Nat Med*. 2010;16:814-20.

19. Mazza G, Al-Akkad W, Rombouts K. Engineering in vitro models of hepatofibrogenesis. *Adv Drug Deliv Rev*. 2017;121:147-157.

20. Mazza G, Al-Akkad W, Telese A, et al. Rapid production of human liver scaffolds for functional tissue engineering by high shear stress oscillation-decellularization. *Sci Rep*. 2017;7:5534.

21. Di Sabatino A, Jackson CL, Pickard KM, et al. Transforming growth factor beta signalling and matrix metalloproteinases in the mucosa overlying Crohn's disease strictures. *Gut*. 2009;58:777-789.

22. Schmittgen TD, Livak KJ. Analyzing real-time PCR data by the comparative C(T) method. *Nat Protoc*. 2008;3:1101-8.

23. Totonelli G, Maghsoudlou P, Garriboli M, et al. A rat decellularized small bowel scaffold that preserves villus-crypt architecture for intestinal regeneration. *Biomaterials*. 2012;33:3401-3410.

24. Nowocin AK, Southgate A, Shurey S, et al. The development and implantation of a biologically derived allograft scaffold. *J Tissue Eng Regen Med*. 2016;10:140-148.

25. Patil PB, Chougule PB, Kumar VK, et al. Recellularization of acellular human small intestine using bone marrow stem cells. *Stem Cells Transl Med*. 2013;2:307-315.

26. Salerno-Goncalves R, Fasano A, Sztein MB. Development of a Multicellular Three-dimensional Organotypic Model of the Human Intestinal Mucosa Grown Under Microgravity. *J Vis Exp*. 2016;(113).

27. Hynes RO. The extracellular matrix: not just pretty fibrils. *Science*. 2009;326:1216-1219.

28. Rescigno M. The intestinal epithelial barrier in the control of homeostasis and immunity. *Trends Immunol*. 2011;32:256-264.

29. Dosh RH, Essa A, Jordan-Mahy N, et al. Use of hydrogel scaffolds to develop an in vitro 3D culture model of human intestinal epithelium. *Acta Biomater*. 2017;62:128-143.

30. Johnson LA, Rodansky ES, Sauder KL, et al. Matrix stiffness corresponding to strictured bowel induces a fibrogenic response in human colonic fibroblasts. *Inflamm Bowel Dis*. 2013;19:891-903.

31. Rieder F, Latella G, Magro F, et al. European Crohn's and Colitis Organisation Topical Review on Prediction, Diagnosis and Management of Fibrostenosing Crohn's Disease. *J Crohns Colitis*. 2016;10:873-885.

32. Kumagai S, Ohtani H, Nagai T, et al. Platelet-derived growth factor and its receptors are expressed in areas of both active inflammation and active fibrosis in inflammatory bowel disease. *Tohoku J Exp Med*. 2001;195:21-33.

33. Kim SH, Turnbull J, Guimond S. Extracellular matrix and cell signalling: the dynamic cooperation of integrin, proteoglycan and growth factor receptor. *J Endocrinol*. 2011;209:139-151.

34. Wu S, Peng H, Li X, et al. Effect of scaffold morphology and cell co-culture on tenogenic differentiation of HADMSC on centrifugal melt electrospun poly (L-lactic acid) fibrous meshes. *Biofabrication*. 2017;9:044106.

**Figure legends**

**Figure 1.** Decellularization of human duodenum by ring-agitation (R-a) protocol. (A) Human duodenum was explanted by Whipple's procedure. It is maintained as a 9 cm long segment (1), which is decellularized by R-a and dissected by scalpel into 3 cm long rings (2) and later into 1 x 0.5 cm squares (3). (B) Macroscopic appearance of a ring at different stages of decellularization by R-a. (C) Histological comparison (original magnification 10x) of native duodenum and duodenum decellularized by R-a by Hematoxylin and Eosin (H&E), Picro-Sirius Red (SR) and Elastin Von Gieson (EVG) staining demonstrating removal of cells and preservation of collagen and elastin in R-a. (D) DNA and (E) collagen quantification was assessed in native duodenum (n=3) and decellularized duodenum (n=3). *$p < 0.01$ versus DNA of duodenum decellularized by R-a protocol.

**Figure 2.** Expression and distribution of ECM proteins. Collagen I (A), Collagen III (C) and Collagen IV (E), fibronectin (G) and laminin (I) staining in native duodenum is seen as fine strands in the lamina propria, *muscularis mucosae* and around the submucosal blood vessels. Collagen I, collagen III and Collagen IV distribution was preserved following decellularization as demonstrated by a staining in the lamina propria and *muscularis mucosae* (B, D, F), and in the submucosa. Fibronectin and laminin staining was retained in the lamina propria and around the submucosal blood vessels (H, J).

**Figure 3.** Ultrastructural characterization of decellularized duodenum. Low magnification (50x) of scanning electron microscopy (SEM) images (A,B) demonstrated preservation of the three-dimensional microanatomy of the mucosal surface and confirmed acellularity in the scaffolds following decellularization (B). Intermediate magnification (150x) (C,D) showed a well-retained

mucosal architecture (D). High magnification (250x) resolution (E,F) demonstrated the preserved 3D structure of villus/crypt ratio (F).

**Figure 4.** Recellularization of human duodenal scaffolds with primary human intestinal myofibroblasts and gene expression of fibrosis markers in primary human intestinal myofibroblasts cultured in standard 2D cultures and repopulated 3D intestinal scaffolds. (A) Human duodenal scaffolds were seeded with primary human intestinal myofibroblasts and bioengineered duodenal tissues were harvested at 7 and 14 days. (B) Haematoxylin and Eosin staining (original magnification 20x) showed that primary human intestinal myofibroblasts were attached on the mucosal surface of the ECM scaffolds at 7 and 14 days. (C) Primary human myofibroblasts were cultured for 12 days in 2D cultures and in 3D scaffolds. This was followed by RNA extraction and qPCR to analyse gene expression of ACTA2, COL1A1, TGF-β1 and MMP-3. Gene expression was normalized to GAPDH. Bars show mean + SD (**/*** $P<0.01/0.005$ n=3 scaffolds per condition).

**Figure 5.** Long-term treatment of primary human intestinal myofibroblasts with TGFβ1 or PDGF-BB in 2D cultures and 3D scaffolds. Cells were treated for 12 days with TGFβ1 or PDGF-BB (A) Haematoxylin and Eosin staining (original magnification 40x) showed that primary myofibroblasts repopulated duodenal 3D scaffolds in control, non-treated cells and TGFβ1- and PDGF-BB-treated cells. Genes showed significant differences between 2D standard culture and 3D scaffolds for (B) ACTA2 expression, (C) COL1A1 expression, (D) TGFβ1 expression, and (E) MMP-3 expression (*/**/*** $P<0.05/0.01/0.005$ n=3). Gene expression was normalized to GAPDH. Data are expressed as mean + SD; n=3 scaffolds per condition.

# Decellularized human gut as a natural 3D-platform for research in intestinal fibrosis

Running Head: Bioengineering of human gut ECM 3D scaffolds

Paolo Giuffrida[1,2*], Marco Curti[1,2*], Walid Al-Akkad,[1] Carin Biel[1], Claire Crowley[3], Luca Frenguelli[1], Andrea Telese[1], Andrew Hall[1], Domenico Tamburrino[4], Gabriele Spoletini[4], Giuseppe Fusai[4], Francesco Paolo Tinozzi[5], Andrea Pietrabissa[5], Gino Roberto Corazza[2], Paolo De Coppi[3,6], Massimo Pinzani[1], Antonio Di Sabatino[1,2], Krista Rombouts[1&], Giuseppe Mazza[1&#]

[1]Regenerative Medicine & Fibrosis Group, Institute for Liver & Digestive Health, University College London, Royal Free Hospital, London, UK

[2]First Department of Internal Medicine, San Matteo Hospital Foundation, University of Pavia, Pavia, Italy.

[3]Stem Cells and Regenerative Medicine Section, Developmental Biology and Cancer Programme, UCL Institute for Child Health, Great Ormond Street Hospital. University College London, London UK.

[4]Division of Surgery, University College London, Royal Free, London, UK.

[5]Department of Surgery, General Surgery II, San Matteo Hospital Foundation, University of Pavia, Pavia, Italy.

[6]Specialist Neonatal and Paediatric Surgery at Great Ormond Street Hospital, London, UK

* PG and MC contributed equally to this manuscript and should be considered joint first authors.

[&] KR and GM contributed equally to this manuscript and should be considered joint senior authors

**Word count**: 3,871

**Abbreviations**: ECM, extracellular matrix; EVG, elastin Van Gieson; H&E, haematoxylin and eosin; IDA, industrial denatured alcohol; MMP, matrix metalloproteinase; PDGF, platelet-derived growth factor; R-a, ring-agitation; SEM, scanning electron microscopy; SR, picro-sirius red; TGF, transforming growth factor; 2D, two-dimensional; 3D, three-dimensional.

[#]**Address for correspondence**: Dr Giuseppe Mazza, Institute for Liver and Digestive Health, UCL Royal Free Campus, Rowland Hill Street, NW3 2PF, London, UK. E-mail: giuseppe.mazza.12@ucl.ac.uk

**Acknowledgements**

This work was supported by the National Institute for Health Research (NIHR), University College London Biomedical Research Centre III (to GM) and the Royal Free Charity (to MP). PDC is supported by NIHR, CC and PDC are supported by the OAK Foundation.

**Author Disclosure Statement**

No competing financial interests exist.

**Summary**

We successfully developed a novel and reproducible protocol designed to "decellularize-recellularize" acellular 3D extracellular matrix (ECM) scaffolds from human intestine. 3D cultures of intestinal myofibroblasts in ECM scaffolds represent a key alterative to 2D cultures on plastic and animal models.

**ABSTRACT**

**Background:** The current methodologies for the identification of therapeutic targets for inflammatory bowel disease (IBD) are limited to conventional two-dimensional (2D) cell cultures and animal models. The use of 3D decellularized human intestinal scaffolds obtained from surgically resected intestine and engineered with human intestinal cells may provide a major advancement in the development of innovative intestinal disease models. Aim of the present study was to design and validate a decellularization protocol for the production of acellular 3D extracellular matrix (ECM) scaffolds from human duodenum.

**Methods:** Scaffolds were characterized by verifying the preservation of the ECM protein composition and 3D architecture of the native intestine and were employed for tissue engineering with primary human intestinal myofibroblasts for up to 14 days.

**Results:** Engrafted cells showed the ability to grow and remodel the surrounding ECM. mRNA expression of key genes involved in ECM turnover was significantly different when comparing primary human intestinal myofibroblasts cultured in 3D scaffolds with these cultured in standard 2D cultures on plastic dishes. Moreover, incubation with key pro-fibrogenic growth factors such as TGFβ1 and PDGF-BB resulted in markedly different effects in standard 2D versus 3D cultures, further emphasizing the importance of using 3D cell cultures.

**Conclusions:** These results confirm the feasibility of 3D culture of human intestinal myofibroblasts in intestinal ECM scaffolds as an innovative platform for disease modelling, biomarker discovery and drug testing in intestinal fibrosis.

**Keywords**: decellularization; human intestinal myofibroblast; 3D ECM scaffold *in vitro* model; tissue regeneration.

## INTRODUCTION

Intestinal fibrosis represents a common consequence of chronic inflammation in inflammatory bowel disease (IBD) and is characterized by the accumulation of fibrillar extracellular matrix (ECM) by activated myofibroblasts.[1] In particular, intestinal fibrosis affects around 40% of patients with Crohn's disease and 5% of patients with ulcerative colitis.[2,3] The lack of an effective medical anti-fibrotic therapy and reliable non-invasive biomarkers still represents an important unmet clinical need in IBD.[2,3].

The traditional platforms used for disease modelling and drug screening in IBD are two-dimensional (2D) cell monolayers cultured on plastic surfaces, and animal models and human organ cultures. However, cells in monolayer cultures tend to de-differentiate because of the high stiffness of the artificial substrate. Thus cellular functions may be affected by the lack of signals from other stromal cells and ECM proteins organized within a tissue-specific 3D architecture.[4] Animal models overcome some of the 2D model limitations by providing physiological features inherent to the gastrointestinal microenvironment, 3D architecture and multicellular complexity. However, most animal models do not fully recapitulate human IBD pathophysiology,[5] are not cost-effective[6] and are burdened by ethical issues.[7] Human organ cultures provide intercellular and cell-ECM networks in a naturally 3D endogenous environment, but they are restricted by low amounts of samples -in particular for the deepest intestinal layers- and by a reduced tissue viability due to poor delivery of oxygen and nutrients, mainly for prolonged cultures.[8] Therefore, due to the high prevalence of gastrointestinal disorders, there is a pressing demand to establish *in vitro* models of human IBD and to develop drug-screening platforms that more accurately recapitulate the complex physiology of the human fibrotic intestine.[9] Tissue engineering has provided new 3D platform technologies, such as organoids, spheroids and scaffolds for the *in vitro* study of pathophysiological mechanisms underlying gastrointestinal disorders. Organoids, which are derived from tissue obtained from biopsies or surgical sections, are 3D cultures which can contain epithelium, and/or pluripotent stem cells, are characterized by high costs of maintenance, lack of proper stromal and ECM components

Formatted: Superscript

in addition to high variability between different laboratories.[10] The use of spheroids allows the growth of human intestinal epithelial cells isolated from mucosal biopsies[11] with a tendency to preserve the region-specific cell differentiation.[12] However, one of the key challenge is the reproducibility of this tool due to size variability.[13] Synthetic intestinal scaffolds can be manufactured with a wide range of materials.[14] However, their main limitation is the absence of the physiological tissue-specific ECM complexity with consequent suboptimal biocompatibility both *in vitro* and *in vivo*.[4,15] Accordingly, biological ECM scaffolds have been successfully obtained by decellularization of human and murine organs, including liver.[16-18] In previous studies we have demonstrated the feasibility of the "decellularization and recellularization" technology of human liver 3D scaffolds which constitutes a valuable platform for liver bioengineering through the repopulation of human liver ECM scaffolds with parenchymal and non-parenchymal liver cells.[16,19] The project herein presented was aimed at the development of a well-defined 3D *in vitro* model based on acellular human gut ECM scaffold engineered with primary human intestinal myofibroblasts and at evaluating the suitability of this construct for disease modelling and target discovery in the high demand area of intestinal fibrosis.

## MATERIALS AND METHODS

**Sources of reagents.** Unless otherwise specified, all reagents were purchased from Sigma.

**Source of human duodena and tissue preparation.** Healthy human duodena (n=5), explanted by Whipple~~'s~~ procedure, were obtained under local ethics from the UCL Royal Free BioBank Ethical Review Committee (NRES Rec Reference: 11/WA/0077). Informed consent was given by each patient taking part in the study. Intestines were washed with 1% PBS solution to clear from blood and luminal contents, dried and frozen at -80 °C for at least 24h.

**Decellularization protocol.** Prior to decellularization, intestines were thawed in a 37°C water bath for 1h, and maintained during the decellularization protocol as long duodenal segments of 9 cm. Once decellularized segments were dissected into 3 cm long rings and later into 1 x 0.5 cm squares The decellularization protocol based on ring agitation (R-a) is shown in Table 1 and Fig. 1A. The resultant tissues were further characterized by employing histological, immunohistochemical studies as well as DNA and collagen quantification.

**Histology.** After the decellularization procedure, samples were fixed for at least 24h in 10% neutral buffered formalin solution (pH 7.4) at room temperature then embedded in paraffin and sectioned at 4 μm. Prior to staining, sections were dewaxed in xylene and rehydrated using a series of graded industrial denatured alcohol (IDA) and water. Tissue sections were stained with Harris's Haematoxylin and Eosin (H&E) (Leica, Germany), Picro-Sirius Red (SR) (Hopkin & Williams) (BDH Chemicals Ltd, Cellpath Ltd) and Miller's Elastic stain with a Picro-Sirius red counter stain (Elastin Van Gieson, EVG) (VWR, Leica, Raymond A Lamb) as previously described.[16]

**Immunohistochemistry.** Sections were incubated in 0.5% Trypsin (MP Biomedical)/0.5% Chymotrypsin (Sigma)/1% Calcium Chloride (BDH) in Tris buffered saline pH 7.6 (TBS) for 30

minutes at 37 °C as previously described.[16]. Slides were then soaked in TBS with 0.04% Tween-20 (Sigma) for 5 minutes, blocked in peroxidase blocking solution (Novocastra) for 5 minutes, washed in TBS for 5 minutes and then incubated for 1h with one of the following primary antibodies: rabbit polyclonal to collagen I (ab34710, 1:200, Abcam), rabbit polyclonal to collagen III (ab7778, 1:500, Abcam), mouse monoclonal to collagen IV (M0785, 1:25, Dako), mouse monoclonal to fibronectin (MAB1937, 1:100, Millipore) and mouse monoclonal to laminin α5-chain (MAB1924, 1:200, Millipore). The slides were then placed for 25 minutes in NovolinkTM post primary (Novocastra), 25 minutes in NovolinkTM polymer solution (Novocastra) and developed with NovolinkTM 3,3′ di-amino-benzidine (Novocastra) with a 5 minutes wash in TBS with 0.04% Tween-20 between each step. Slides were counterstained with Mayer's Haematoxylin (Sigma) for 3 minutes. All sections were dehydrated in graded IDA and xylene and were mounted with DPX (Leica biosystems); cover slipped and observed using a Zeiss Axioskop 40. Images were captured with an Axiocam IcC5 using Zeiss Axiovision (verison 4.8.2). All images were analyzed and enhanced using Fiji v1.49d (ImageJ Jenkins server).

**DNA quantification.** To assess total DNA content within native tissue and acellular matrices, the DNeasy Blood and Tissue kit was used according to the manufacturer's manual (Qiagen) and as described previously.[16,20] Briefly, specimens were digested with Proteinase K overnight. DNA samples were purified using buffers provided by the company and measured spectrophotometrically (Nanodrop, Thermo Scientific, US). Optical densities at 260 nm and 280 nm were used to estimate the purity and yield of nucleic acids.

**Collagen quantification.** The collagen content of native tissue and decellularized tissue was quantified as described previously[16] using the total collagen assay kit according to the manufacturer's manual (QuickZyme Biosciences, The Netherlands). Briefly, samples were hydrolyzed in 6M HCl at 95°C for 20h, the hydrolysates were mixed with a chromogen solution

staining the hydroxyproline residues and color was developed at 60°C for 1h. The absorbance for each sample was determined at 555 nm using a FLUOstar Omega microplate reader (BMG labtech, Germany) and the collagen quantity was calculated by employing a standard curve of pure collagen hydrolysates.

**Scanning Electron Microscopy (SEM).** Samples were fixed in 2.5% glutaraldehyde in 0.1 M phosphate buffer and left for 24h at 4°C, as previously described.[16] Briefly, following washing with 0.1 M phosphate buffer, samples were cut into segments of approximately 1 cm length and cryoprotected in 25% sucrose, 10% glycerol in 0.05 M PBS (pH 7.4) for 2h, then fast frozen in Nitrogen slush and fractured at approximately − 160°C. Next, samples were placed back into the cryoprotectant at room temperature and allowed to thaw. After washing in 0.1 M phosphate buffer (pH 7.4), the material was fixed in 1% $OsO_4$ / 0.1 M phosphate buffer (pH 7.3) at 3°C for 1½h and washed again in 0.1 M phosphate buffer (pH 7.4). After rinsing with distilled water, specimens were dehydrated in a graded ethanol-water series to 100% ethanol; critical point dried using $CO_2$ and finally mounted on aluminium stubs using sticky carbon taps. The fractured material was mounted to present fractured surfaces across the parenchyma to the beam and coated with a thin layer of Au/Pd (approximately 2 nm thick) using a Gatan ion beam coater. Images were recorded with a 7401 FEG scanning electron microscope (Jeol, USA).

**Sterilization of decellularized tissue.** Prior to in vitro cell seeding, intestinal cubes were sterilized by immersion in 0.1%PAA-4%EtOH for 45 minutes, followed by a washing step in sterile 1X PBS for 15 minutes. During both steps intestinal cubes were agitated using the Orbit M60 Digital Microtube Shaker at 900 rpm.

**Human intestinal myofibroblast isolation and culture.** Cells were isolated as previously described.[21] Briefly, the epithelial layer was removed by 1 mM EDTA for two 30 minutes periods at

37°C. After EDTA treatment, intestinal mucosal samples were denuded of epithelial cells, and were subsequently cultured at 37°C in a humidified $CO_2$ incubator in Dulbecco's modified Eagle's medium (DMEM) supplemented with 20% fetal calf serum, 100 U/ml penicillin, 100 mg/ml streptomycin, 50 mg/ml gentamycin and 2.5 mg/ml amphotericin. During culture, numerous cells appeared both in suspension and adhered to the culture dish. The cells in suspension were removed every 24–72 h, and the denuded mucosal tissue was maintained in culture for up to 6 weeks. Established colonies of myofibroblasts were seeded into 25 $cm^2$ culture flasks and cultured in DMEM supplemented with 20% FCS and antibiotics. At confluence, the cells were passaged using trypsin-EDTA in a 1:2 to 1:3 split ratio. Cells were grown up to passage 7 – 10 before the final concentration was reached to perform experiments.

**Repopulation and culture of engineered human intestine.** Sterilized human gut scaffolds were kept overnight in complete medium [day -1]. Myofibroblasts were trypsinized and then re-suspended at a final concentration of 25,000 cells/µl. Scaffolds were reseeded with 20 µl of cell-containing medium (0.5 million cells/scaffold) by using the drop-on technique, as previously described.[16] Seeded scaffolds were kept for 2h in a humidified incubator at 37°C with 5% $CO_2$ allowing cell attachment followed by the addition of the complete culture medium [day 0]. The culture medium was changed at day 1 and afterwards every 3 days. At days 7 and 14 following seeding, the scaffolds were placed in 10% formalin and assessed by histology analysis.

**2D culture and 3D culture long-term treatment.** In order to compare myofibroblast cell behavior both 2D and 3D experiments were performed in parallel. At day 0, myofibroblasts (150,000 per well) were plated on a 6 well cell culture dish (Greiner Bio-one) or reseeded in intestinal scaffolds (0.5 million cells/scaffold). Long term treatment with platelet-derived growth factor (PDGF)-BB (10 ng/ml, PeproTech) or transforming growth factor (TGF)-β1 (10 ng/ml, R&D systems) was

started at day -1 up to day 12. Culture media plus stimuli was refreshed every 3 days. At day 12, scaffolds were snap frozen and stored at -80°C until RNA extraction.

**RNA extraction and quantitative real-time PCR (qPCR).** RNA was isolated from myofibroblasts cultured in scaffolds by using RNeasy® Plus Micro Kit (Qiagen) according to the manufactures' protocol. First the scaffolds were disrupted and homogenized by shaking for 5 min at 50Hz (Qiagen TissueLyser LT) with a 5 mm and a 7 mm stainless steel beats (Qiagen) in 350 µl Buffer RLT plus. RNA concentration and purity were measured with Nanodrop spectrophotometer (Thermo Scientific). RNA was isolated from the myofibroblasts cultured in 2D by using RNeasy® Mini Kit according to the manufactures' protocol. Complementary DNA (cDNA) was synthesized using the following reaction mix: MultiScribe reverse transcriptase, random primers, dNTP mix and RNase inhibitor (Applied Biosystems) and reverse transcription was performed with a Q Cycler II (Quanta Biotech). qPCR was performed by using Taqman gene assays (Applied Biosystems) for the following genes: GAPDH (Hs02758991_g1), ACTA2 (Hs00426835_g1), COL1A1 (Hs00164004_m1), TGFβ1 (Hs00998133_m1) and matrix metalloproteinase MMP-3 (Hs00968305_m1). The comparative Ct method was used to quantify relative gene expression, using Glyceraldehyde 3-phosphate dehydrogenase (GADPH) as internal control as previously described.[20,22]

**Statistical analysis.** Data were analyzed with the GraphPad Prism statistical PC program (GraphPad Software, San Diego, CA) using Anova or Student's t-test. Results were expressed as mean ± SEM or standard deviation (SD). Two-tailed p values less than 0.05 were considered statistically significant.

## RESULTS

**Decellularization of human duodenum.** Decellularization of the duodenum was completed within one week by employing the R-a protocol (Table 1). While progressing through the decellularization process, tissue rings became increasingly translucent (Fig. ~~2A~~1B). The R-a protocol is characterized by applying a combination of four different cell-damaging factors: (*i*) freezing/thawing, (*ii*) mechanical agitation by employing shaker ~~or roller~~, (*iii*) osmotic stress, i.e. distilled water and PBS, to allow cell lysis, and (*iv*) the detergent sodium deoxycholate to remove debris (Table 1). Histological assessment by H&E and SR staining showed no evidence of nuclear or cellular material in the decellularized 3D duodenum scaffolds (Fig. ~~2B~~1C). Moreover, the overall gut architecture appeared fully preserved as shown by SR staining for collagens and EVG staining for elastin (Fig. ~~2B~~1C). The efficacy of the R-a protocol was confirmed by the absence of quantifiable DNA material (Fig. ~~2C~~1D) as the DNA quantification demonstrated a significant DNA reduction in decellularized gut (mean 42.6 ± 11.6 ng/mg) in comparison to native gut (mean 846.4 ± 149.9 ng/mg) ($p<0.01$). Furthermore, no significant difference in collagen content was observed between decellularized gut (mean 44.3 ± 11.4 ng/mg) and native gut tissue (mean 57.6 ± 15.8 ng/mg) (Fig. ~~2D~~1E).

**Duodenal tissue scaffold characterization.** To assess the preservation of ECM components, the ECM expression and distribution of different ECM components were evaluated by immunohistochemistry (Fig. ~~3~~2A-J). Five key structural ECM proteins, i.e. collagen I (Fig. ~~3~~2B), collagen III (Fig. ~~3~~2D), collagen IV (Fig. ~~3~~2F), fibronectin (Fig. ~~3~~2H) and laminin (Fig. ~~3~~2J) were fully preserved following decellularization in comparison to native duodenal tissue (Fig. ~~3~~2A,C,E,G,I). Furthermore, the distribution of each ECM protein within the duodenal scaffoldconfirmed the complete preservation of the architecture of the native duodenal tissue.

**Ultrastructural characterization of decellularized human duodenum.** SEM was performed to further investigate the effects of decellularization on the 3D-architecture and microstructure of the ECM (Fig. ~~4~~3A-F). At low magnification, the 3D architecture of duodenal scaffolds (Fig. ~~4~~3B) appeared to be preserved in comparison to the architecture of the native tissue (Fig. ~~4~~3A). At intermediate and high magnification, in particular, the 3D-microstructure of villus/crypt ratio was demonstrated (Fig. ~~4~~3D,F) and comparable to that of the native duodenal tissue (Fig. ~~4~~3C,E).

**Bioengineering of human duodenal scaffolds with primary human intestinal myofibroblasts.** In order to evaluate the *in vitro* biocompatibility, human duodenal ECM scaffolds were reseeded with primary human intestinal myofibroblasts (Fig. ~~5~~4A). The repopulated scaffolds were evaluated after 7 days up to 14 days of culture. H&E staining showed a progressive engraftment of primary human intestinal myofibroblasts into the scaffold over 14 days (Fig. ~~5~~4B).

**Primary human intestinal myofibroblasts bioengineered in human duodenal 3D scaffolds display a different gene expression compared to standard 2D culture conditions.** Gene expression in primary human intestinal myofibroblasts was evaluated by culturing cells in standard 2D culture conditions and 3D intestinal scaffolds (Fig. ~~5~~4C). Gene expression was evaluated by performing qPCR for the following markers ACTA2, COL1A1, TGF-β1, and MMP-3 typical of tissue wound healing/fibrogenesis. As illustrated in Figure ~~5~~4C, significant differences in gene expression were detected comparing 2D versus 3D cultures. Specifically, ACTA2 and COL1A1 mRNA expression was more than 5 times higher in myofibroblasts cultured in 2D compared with fibroblasts cultured in 3D intestinal scaffolds (***$p<0.005$, 2D vs 3D). The expression of TGF-β1 was four times higher in fibroblasts cultured on intestinal scaffolds compared to myofibroblasts cultured in standard 2D culture conditions (**$p<0.01$, 2D vs 3D). MMP-3 expression was two times higher in the myofibroblasts cultured engrafting 3D intestinal scaffolds compared to myofibroblasts cultured in 2D culture (*** $p<0.005$, 2D vs 3D).

**Long term treatment with TGF-β1 or PDGF-BB.** In order to mimic a microenvironment closer to that of chronic intestinal disease, the bioengineered constructs were subjected to treatment for up to 12 days with TGFβ1 or PDGF-BB followed by histological analysis and assessment of gene expression and compared to standard 2D cultures. Cells repopulated in 3D scaffolds showed a stronger engraftment and intra-scaffold spreading with long-term PDGF-BB treatment (Fig. ~~6~~5A) in comparison to control condition. TGF-β1 treatment induced a significant up-regulation of ACTA2 (*** $p<0.005$ vs control) only in 3D cultured myofibroblasts when compared to control (Fig. 6B). Cells cultured in 2D as well as 3D and long-term treated with PDGF-BB did not show any significant difference in ACTA2 mRNA expression (Fig. ~~6~~5B). COL1A1 mRNA expression was significantly up-regulated upon TGF-β1 treatment in both 2D and 3D cultured fibroblasts in comparison to non-treated control cells (*** $p<0.005$ and ** $p<0.01$, respectively) (Fig. ~~6~~5C). TGF-β1 expression did not significantly differ upon long-term treatment with TGF-β1 or PDGF-BB in standard 2D conditions, but was significantly up-regulated upon exogenous TGF-β1 treatment in 3D compared to the non-treated, control 3D culture (*** $p<0.005$) and 2D versus 3D treated cells, respectively (*** $p<0.005$ respectively) (Fig. ~~6~~5D). MMP-3 mRNA expression in 2D cultured myofibroblasts treated with TGF-β1 was significantly decreased compared to non-treated control cells in 2D cultured (Fig, ~~7~~5D, * $p<0.05$ control vs TGFβ1 treated in 2D). In 3D cultured TGFβ1-treated myofibroblasts, MMP-3 expression was significantly up-regulated in comparison to 2D culture treated cells (Fig. ~~6~~5E, ** $p<0.01$ TGFβ1 treatment 2D vs 3D). Long-term treatment with PDGF-BB did not affect MMP-3 mRNA expression (Fig.~~7~~5E).

## DISCUSSION

We report the successful development of a novel and reproducible methodology for the decellularization of human duodenum leading to the production of human intestinal 3D ECM scaffolds. This achievement represents an important basis for tissue engineering of the gut with the aim to develop research platforms for disease modelling, drug target and biomarker discovery in addition to drug efficacy testing in human intestinal fibrosis.

Decellularization of the gut of several animals, including rat and pig, had been previously reported with data demonstrating the conservation of key properties of connective tissue and vasculature ~~(22, 23)~~.[23,24] Furthermore, the decellularization of human intestine had been already reported for regenerative medicine applications ~~(24)~~.[25] Differently, our primary aim was to decellularize human duodenal tissue and then proceed to the recellularization of the 3D scaffolds using human primary intestinal myofibroblasts to develop 3D models for the study of intestinal fibrosis. This latter development is highly awaited to overcome the experimental limitations of the currently available platforms, including standard 2D culture models, animal models, organoids, spheroids and synthetic scaffolds.

An important feature of the proposed decellularization procedure is the possibility of obtaining 3D intestinal ECM scaffolds from specimens obtained by routine surgical resections thus allowing a more widespread application in hospitals and academic centres. This natural 3D-platform represents a simple method based on four different cell-damaging factors, freezing/thawing, mechanical agitation, osmotic stress and the detergent sodium deoxycholate. Hundreds of 3D ECM scaffolds, 1 x 0.5 $cm^2$, are obtained from a gut ring and could be used for several experiments. However, the main limitation of this method is the training on decellularization-recellularization technique which might constitute a gap for other research groups. Another challenge might be difficulty in obtaining significantly long gut rings for research groups with no access to surgical specimens from Whipple procedures.

Formatted: Superscript
Formatted: Superscript
Formatted: Superscript

The use of an ECM platform in which biochemical and biomechanical ECM features are maintained is crucial for the development of tissue bioengineering aimed at regenerative and modelling purposes. Accordingly, the current trend is to employ different ECM substrates in 3D configuration to improve the physiological microenvironment to study human cell behavior ~~(18)~~.[19] For example, recently published work has focused on a 3D organotypic model of human intestinal mucosa by using a bioreactor and collagen gel ~~(25)~~.[26] The results of the present study provides, for the first time, evidence of an efficient decellularization-recellularization of human 3D intestinal scaffolds which are characterized by the preservation of the key features of human intestinal ECM modulating fundamental cellular functions, such as differentiation, induction and maintenance of phenotype ~~(26)~~.**Error! Reference source not found.** In particular, the decellularization protocol showed the preservation of both collagen and elastin distribution. In terms of topographic distribution, the retention of the five key ECM proteins, namely collagen I, III and IV, fibronectin and laminin was observed by immunohistochemistry in the lamina propria, along the *muscularis mucosae* and around the submucosal blood vessels without significant differences with their distribution in the native tissue. In addition, SEM demonstrated that the 3D-architecture of mucosal ECM, in particular the villus/crypt ratio, was preserved. A key effort of this study was to evaluate in *vitro* biocompatibility of the scaffold when repopulated by organ-specific cells such as human primary intestinal myofibroblasts ~~(15, 20, 27)~~.[16,21].**Error! Reference source not found.** Intestinal myofibroblasts demonstrated an effective engraftment in their typical anatomical location. In particular, they were able to engraft not only into the lamina propria, where the cells originally were isolated, but also into the submucosa and in the muscle layer. Moreover, the expression profile of phenotype-specific markers for primary human intestinal myofibroblasts indicated that the engrafted cells maintained higher cellular differentiation features as well as a less activated phenotype following prolonged culture in 3D scaffolds when compared to the same cell preparation grown in standard 2D-plastic conditions. Indeed, the mRNA expression of key pro-fibrogenic and ECM remodelling genes (ACTA2, COL1A1, TGFβ1 and MMP-3) showed a remarkable difference between 3D scaffold

Formatted: Superscript

Formatted: Superscript

cultures and 2D standard culture conditions, thus confirming that the phenotype of primary cells can be dramatically affected by *in vitro* culture employing either artificial and non-physiological high stiffness substrates ~~(19, Dosh RH et al. Acta Biomater 2017;62:128-143).~~[20] **Error! Reference source not found.** Along these lines, and similarly to what observed comparing cultures of human hepatic stellate cells in human liver 3D ECM scaffolds versus cultures of the same cells on plastic dishes,[20] it is evident that the upregulation of key pro-fibrogenic genes such as ACTA2 and COL1A1 is largely artificial and dependent on the high stiffness of the substrate rather than a physiological or pathophysiological response to growth factors such as TGF-β1.[30] The parallel higher TGF-β1 and MMP-3 gene expression observed in the 3D scaffolds compared to the 2D cultures further highlights and complete the divergence between the two types of culture platforms. In addition, the differences in baseline gene expression observed in different culture conditions are likely to condition the changes in gene expression following stimulation with TGF-β1. ~~we demonstrated that the expression of pro-fibrogenic genes such as ACTA2 and COL1A1 was down-regulated in 3D scaffolds, thus highlighting the role of native microenvironment in reducing cell activation compared to 2D rigid substrate cultures. In contrast, both ECM remodelling gene expression of TGF-β1 and MMP-3 was increased in myofibroblasts cultured in 3D scaffolds further emphasizing an ECM specific regulation of specific gene expression. This does corroborate previous data showing that fibroblasts have a higher expression of ACTA2 and collagens when cultured on stiff matrix or rigid substrate such as standard 2D plastic dishes (28).~~

To further investigate the use of tissue-specific human ECM scaffolds for fibrostenotic IBD, we treated intestinal myofibroblasts cultured in 3D duodenal scaffolds and in 2D standard conditions with key pro-fibrogenic growth factors such as TGF-β1 and PDGF-BB ~~(29).~~[31] Stimulation with both pro-fibrogenic mediators resulted in different effects on the expression of target mRNAs when comparing myofibroblasts cultured in 3D or 2D cultures. Again, these results emphasize the specific interaction between cells and the microenvironment, i.e. 2D versus 3D, and the effect of pro-fibrotic mediators. It is very plausible that the response to both TGF-β1 and PDGF-BB

**Formatted:** Superscript

**Formatted:** Superscript

**Formatted:** Superscript

observed in fibroblasts cultured in 3D scaffolds is closer to the cellular *in vivo* response and also by taking into account the absence of specific integrin/cytoskeletal interactions in 2D which is necessary for a correct growth factor intracellular signalling ~~(30, 31)~~.[32,33] Interestingly, TGF-β1 mRNA expression, already induced in 3D cultures in comparison to 2D cultures, is further up-regulated in 3D scaffolds by prolonged treatment of the cells with exogenous TGF-β1. Similar results were obtained for MMP-3 mRNA expression when cultured in 3D scaffolds compared to 2D cultures on plastic. This confirms that MMP-3 mRNA and protein expression are artificially down-regulated in myofibroblasts grown on rigid high stiffness 2D plastic substrata ~~(20)~~,[21] whereas this study demonstrates that MMP-3 gene expression can be further up-regulated by exogenous TGF-β1 stimulation in human 3D scaffolds cultures. Overall, these data highlight remarkable differences in cell biology when cells are cultured in their own native 3D ECM scaffold and when compared with standard 2D culture conditions. Therefore, the novel *in vitro* 3D model described in the present study further adds accuracy and validity to the search for molecular targets of intestinal fibrosis. Similarly to co-culture of distinct cell types in other 3D scaffolds,[34] our 3D-platform could also have potential implications in investigating interactions between myofibroblasts and other intestinal cell types, such as epithelial cells and immune cells, in sequential, which might clarify the complexity of disease modelling and screen drugs in IBD more-in-depth. However, this lies outside of the aim of the present study.

Formatted: Superscript
Formatted: Superscript
Formatted: Superscript
Formatted: Superscript

In conclusion, the present study describes the development of a novel effective protocol for generating 3D tissue-specific ECM scaffolds to improve the knowledge on the pathogenesis of intestinal fibrosis including fibrostenotic IBD, to predict drug efficacy or toxicity, to discover biomarkers, and to reduce developmental costs of current models, i.e. 2D cultures and animal models.

**Contributors**

PG, WAA, PDC, MP, ADS, KR and GM designed the study. PG, MC, WAA, CB, CC, LF, AT and AH collected data. WAA, MP, ADS, DT, GS, GF, FPT, AP and GM provided material. All authors analyzed and interpreted the data. PG, MC and CB did the statistical analyses. PG, MC, CB, GRC, MP, ADS, KR, and GM wrote the manuscript. All authors approved the final report.

**References**


1. Lenti MV, Di Sabatino A. Intestinal fibrosis. *Mol Aspects Med*. 2019;65:100-109.
2. Rieder F, Bettenworth D, Ma C, et al. An expert consensus to standardise definitions, diagnosis and treatment targets for anti-fibrotic stricture therapies in Crohn's disease. *Aliment Pharmacol Ther*. 2018;48:347-357.
3. Giuffrida P, Pinzani M, Corazza GR, et al. Biomarkers of intestinal fibrosis - one step towards clinical trials for stricturing inflammatory bowel disease. *United European Gastroenterol J*. 2016;4:523-530.
4. Pereira JF, Awatade NT, Loureiro CA, et al. The third dimension: new developments in cell culture models for colorectal research. *Cell Mol Life Sci*. 2016;73:3971-3989.
5. Macdonald TT. Inside the microbial and immune labyrinth: totally gutted. *Nat Med*. 2010;16:1194-1195.
6. Huh D, Matthews BD, Mammoto A, et al. Reconstituting organ-level lung functions on a chip. *Science*. 2010;328:1662-1668.
7. Elliott NT, Yuan F. A review of three-dimensional in vitro tissue models for drug discovery and transport studies. *J Pharm Sci*. 2011;100:59-74.
8. Al-Lamki RS, Bradley JR, Pober JS. Human Organ Culture: Updating the Approach to Bridge the Gap from In Vitro to In Vivo in Inflammation, Cancer, and Stem Cell Biology. *Front Med (Lausanne)*. 2017;4:148.
~~7.~~
~~8.~~9. Benam KH, Dauth S, Hassell B, et al. Engineered in vitro disease models. *Annu Rev Pathol*. 2015;10:195-262.
~~9.~~10. Dedhia PH, Bertaux-Skeirik N, Zavros Y, et al. Organoid Models of Human Gastrointestinal Development and Disease. *Gastroenterology*. 2016;150:1098-1112.
~~10.~~11. VanDussen KL, Marinshaw JM, Shaikh N, et al. Development of an enhanced human gastrointestinal epithelial culture system to facilitate patient-based assays. *Gut*. 2015;64:911-920.
~~11.~~12. Ray K. Intestinal tract. Patient-derived intestinal spheroids--culturing the gut. *Nat Rev Gastroenterol Hepatol*. 2014;11:516.
~~12.~~13. Fennema E, Rivron N, Rouwkema J, et al. Spheroid culture as a tool for creating 3D complex tissues. *Trends Biotechnol*. 2013;31:108-115.
~~13.~~14. Costello CM, Hongpeng J, Shaffiey S, et al. Synthetic small intestinal scaffolds for improved studies of intestinal differentiation. *Biotechnol Bioeng*. 2014;111:1222-1232.


Formatted: Font: 12 pt

Formatted: Font: 12 pt

14.15. Chan BP, Leong KW. Scaffolding in tissue engineering: general approaches and tissue-specific considerations. *Eur Spine J*. 2008;17 Suppl 4:467-79.

15.16. Mazza G, Rombouts K, Rennie Hall A, et al. Decellularized human liver as a natural 3D-scaffold for liver bioengineering and transplantation. *Sci Rep*. 2015;5:13079.

16.17. Mazza G, Simons JP, Al-Shawi R, et al. Amyloid persistence in decellularized liver: biochemical and histopathological characterization. *Amyloid*. 2016;23:1-7.

17.18. Uygun BE, Soto-Gutierrez A, Yagi H, et al. Organ reengineering through development of a transplantable recellularized liver graft using decellularized liver matrix. *Nat Med*. 2010;16:814-20.

18.19. Mazza G, Al-Akkad W, Rombouts K. Engineering in vitro models of hepatofibrogenesis. *Adv Drug Deliv Rev*. 2017;121:147-157.

19.20. Mazza G, Al-Akkad W, Telese A, et al. Rapid production of human liver scaffolds for functional tissue engineering by high shear stress oscillation-decellularization. *Sci Rep*. 2017;7:5534.

20.21. Di Sabatino A, Jackson CL, Pickard KM, et al. Transforming growth factor beta signalling and matrix metalloproteinases in the mucosa overlying Crohn's disease strictures. *Gut*. 2009;58:777-789.

21.22. Schmittgen TD, Livak KJ. Analyzing real-time PCR data by the comparative C(T) method. *Nat Protoc*. 2008;3:1101-8.

22.23. Totonelli G, Maghsoudlou P, Garriboli M, et al. A rat decellularized small bowel scaffold that preserves villus-crypt architecture for intestinal regeneration. *Biomaterials*. 2012;33:3401-3410.

23.24. Nowocin AK, Southgate A, Shurey S, et al. The development and implantation of a biologically derived allograft scaffold. *J Tissue Eng Regen Med*. 2016;10:140-148.

24.25. Patil PB, Chougule PB, Kumar VK, et al. Recellularization of acellular human small intestine using bone marrow stem cells. *Stem Cells Transl Med*. 2013;2:307-315.

25.26. Salerno-Goncalves R, Fasano A, Sztein MB. Development of a Multicellular Three-dimensional Organotypic Model of the Human Intestinal Mucosa Grown Under Microgravity. *J Vis Exp*. 2016;(113).

26.27. Hynes RO. The extracellular matrix: not just pretty fibrils. *Science*. 2009;326:1216-1219.

27.28. Rescigno M. The intestinal epithelial barrier in the control of homeostasis and immunity. *Trends Immunol*. 2011;32:256-264.

28.29. Dosh RH, Essa A, Jordan-Mahy N, et al. Use of hydrogel scaffolds to develop an in vitro 3D culture model of human intestinal epithelium. *Acta Biomater*. 2017;62:128-143.

~~29.~~30. Johnson LA, Rodansky ES, Sauder KL, et al. Matrix stiffness corresponding to strictured bowel induces a fibrogenic response in human colonic fibroblasts. *Inflamm Bowel Dis*. 2013;19:891-903.

~~30.~~31. Rieder F, Latella G, Magro F, et al. European Crohn's and Colitis Organisation Topical Review on Prediction, Diagnosis and Management of Fibrostenosing Crohn's Disease. *J Crohns Colitis*. 2016;10:873-885.

~~31.~~32. Kumagai S, Ohtani H, Nagai T, et al. Platelet-derived growth factor and its receptors are expressed in areas of both active inflammation and active fibrosis in inflammatory bowel disease. *Tohoku J Exp Med*. 2001;195:21-33.

33. Kim SH, Turnbull J, Guimond S. Extracellular matrix and cell signalling: the dynamic cooperation of integrin, proteoglycan and growth factor receptor. *J Endocrinol*. 2011;209:139-151.

~~32.~~34. Wu S, Peng H, Li X, et al. Effect of scaffold morphology and cell co-culture on tenogenic differentiation of HADMSC on centrifugal melt electrospun poly (L-lactic acid) fibrous meshes. *Biofabrication*. 2017;9:044106.

**Formatted:** English (United Kingdom)

**Figure legends**

**Figure 1.** Decellularization of human duodenum by ~~R~~ring-agitation (R-a) protocol. (A) Human duodenum was explanted by Whipple's procedure. It is maintained as a 9 cm long segment (~~A~~1), which is decellularized by R-a and dissected by scalpel into 3 cm long rings (~~B~~2) and later into 1 x 0.5 cm squares (~~C~~3).

~~**Figure 2.** Decellularization of human duodenum.~~ (~~A~~B) Macroscopic appearance of a ring at different stages of decellularization by ~~ring-agitation (~~R-a~~) protocol~~. (~~B~~C) Histological comparison (original magnification 10x) of native duodenum and duodenum decellularized by R-a ~~protocol~~ by Hematoxylin and Eosin (H&E), Picro-Sirius Red (SR) and Elastin Von Gieson (EVG) staining demonstrating removal of cells and preservation of collagen and elastin in R-a. (~~C~~D) DNA and (~~D~~E) collagen quantification was assessed in native duodenum (n=3) and decellularized duodenum (n=3). *p < 0.01 versus DNA of duodenum decellularized by R-a protocol.

**Figure ~~3~~2.** Expression and distribution of ECM proteins. Collagen I (A), Collagen III (C) and Collagen IV (E), fibronectin (G) and laminin (I) staining in native duodenum is seen as fine strands in the lamina propria, *muscularis mucosae* and around the submucosal blood vessels. Collagen I, collagen III and Collagen IV distribution was preserved following decellularization as demonstrated by a staining in the lamina propria and *muscularis mucosae* (B, D, F), and in the submucosa. Fibronectin and laminin staining was retained in the lamina propria and around the submucosal blood vessels (H, J).

**Figure ~~4~~3.** Ultrastructural characterization of decellularized duodenum. Low magnification (50x) of scanning electron microscopy (SEM) images (A,B) demonstrated preservation of the three-dimensional microanatomy of the mucosal surface and confirmed acellularity in the scaffolds

following decellularization (B). Intermediate magnification (150x) (C,D) showed a well-retained mucosal architecture (D). High magnification (250x) resolution (E,F) demonstrated the preserved 3D structure of villus/crypt ratio (F).

**Figure ~~5~~4.** Recellularization of human duodenal scaffolds with primary human intestinal myofibroblasts and gene expression of fibrosis markers in primary human intestinal myofibroblasts cultured in standard 2D cultures and repopulated 3D intestinal scaffolds. (A) Human duodenal scaffolds were seeded with primary human intestinal myofibroblasts and bioengineered duodenal tissues were harvested at 7 and 14 days. (B) Haematoxylin and Eosin staining (original magnification 20x) showed that primary human intestinal myofibroblasts were attached on the mucosal surface of the ECM scaffolds at 7 and 14 days. (C) Primary human myofibroblasts were cultured for 12 days in 2D cultures and in 3D scaffolds. This was followed by RNA extraction and qPCR to analyse gene expression of ACTA2, COL1A1, TGF-β1 and MMP-3. Gene expression was normalized to GAPDH. Bars show mean + SD (**/*** P<0.01/0.005 n=3 scaffolds per condition).

**Figure ~~6~~5.** Long-term treatment of primary human intestinal myofibroblasts with TGFβ1 or PDGF-BB in 2D cultures and 3D scaffolds. Cells were treated for 12 days with TGFβ1 or PDGF-BB (A) Haematoxylin and Eosin staining (original magnification 40x) showed that primary myofibroblasts repopulated duodenal 3D scaffolds in control, non-treated cells and TGFβ1- and PDGF-BB-treated cells. Genes showed significant differences between 2D standard culture and 3D scaffolds for (B) ACTA2 expression, (C) COL1A1 expression, (D) TGFβ1 expression, and (E) MMP-3 expression (*/**/*** P<0.05/0.01/0.005 n=3). Gene expression was normalized to GAPDH. Data are expressed as mean + SD; n=3 scaffolds per condition.

**Table 1.** Decellularization protocol based on ring-agitation (R-a).

| Day | Step | Reagent | Time | Temperature | Agitation system |
|---|---|---|---|---|---|
| 0 | 1 | $dH_2O$ | 20 min x 6 | RT | + |
| | 2 | $dH_2O$ | 5h | RT | + |
| | 3 | $dH_2O$ | 90 min | 4 °C | + |
| | 4 | $dH_2O$ | Overnight | 4 °C | - |
| 1 | 5 | Cut in three 3 cm rings | | RT | - |
| | 6 | PBS | 20 min | RT | + |
| | 7 | SDC 4% | 2h | RT | + |
| | 8 | $dH_2O$ | 2h | RT | + |
| | 9 | SDC 4% | 2h | RT | + |
| | 10 | PBS | 30 min | RT | + |
| | 11 | PBS | Overnight | 4 °C | - |
| 2 | 12 | SDC 4% | 5h | RT | + |
| | 13 | PBS | 30 min | RT | + |
| | 14 | PBS | 30 min | RT | + |
| | 15 | PBS | 1h | RT | + |
| | 16 | SDC 4% | Overnight | RT | + |
| 3 | 17 | PBS | 2h | RT | + |
| | 18 | SDC 4% | 7h | RT | + |
| | 19 | PBS | 30 min | RT | + |
| | 20 | PBS | Overnight | RT | + |
| 4 | 21 | SDC 4% | 7h | RT | + |
| | 22 | PBS | Overnight | RT | + |
| 5 | 23 | SDC 4% | 7h | RT | + |
| | 24 | PBS | Overnight | RT | + |
| 6 | 25 | SDC 4% | 7h | RT | + |
| | 26 | PBS | 30 min | RT | + |
| | 27 | PBS | Overnight | RT | + |
| 7 | 28 | PBS | Storage | 4 °C | - |

$dH_2O$, distilled water; RT, room temperature; SDC, sodium deoxycholate; +, R-a with Labnet Orbit M60 microtube shaker.

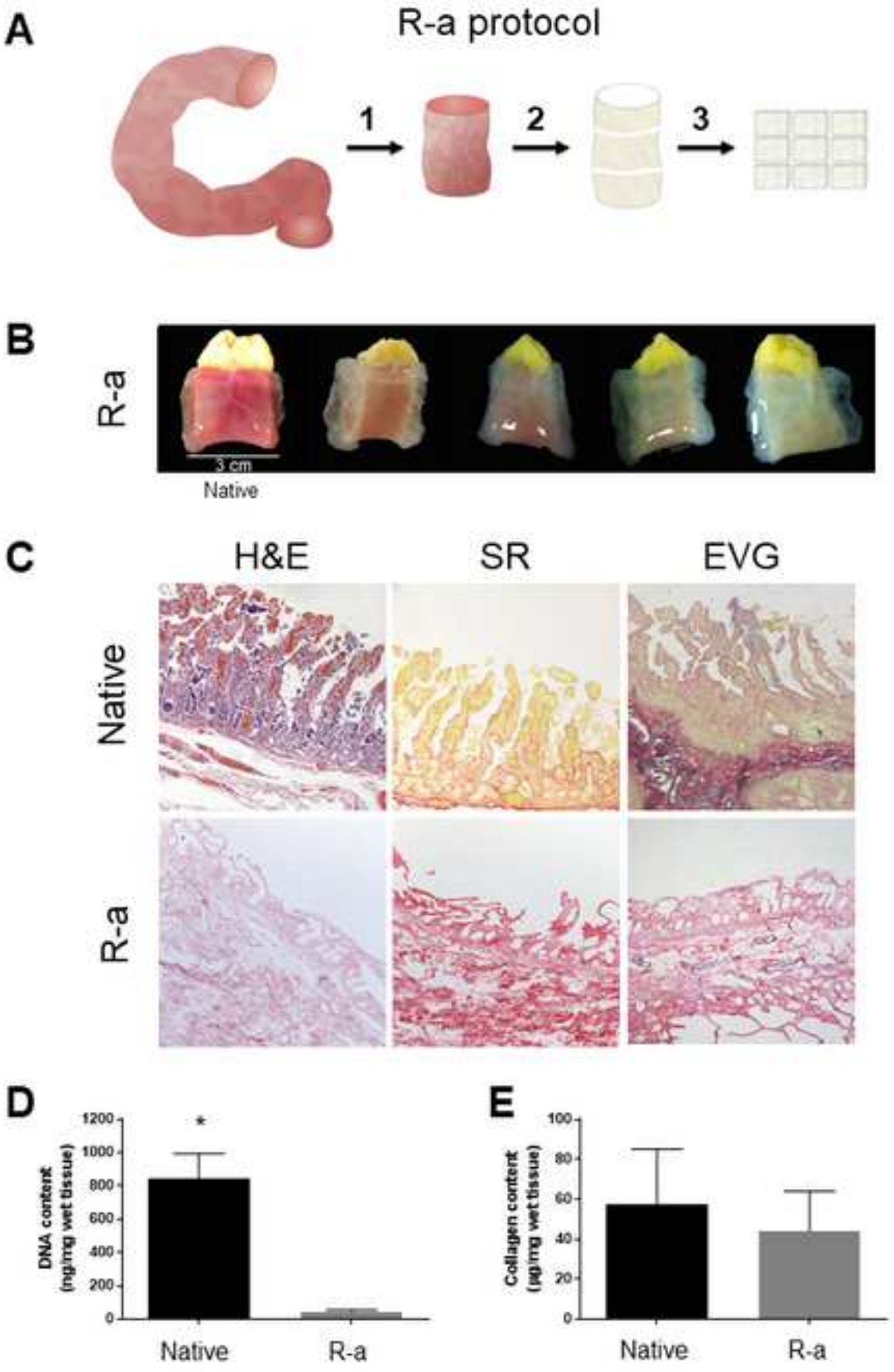


Figure 1

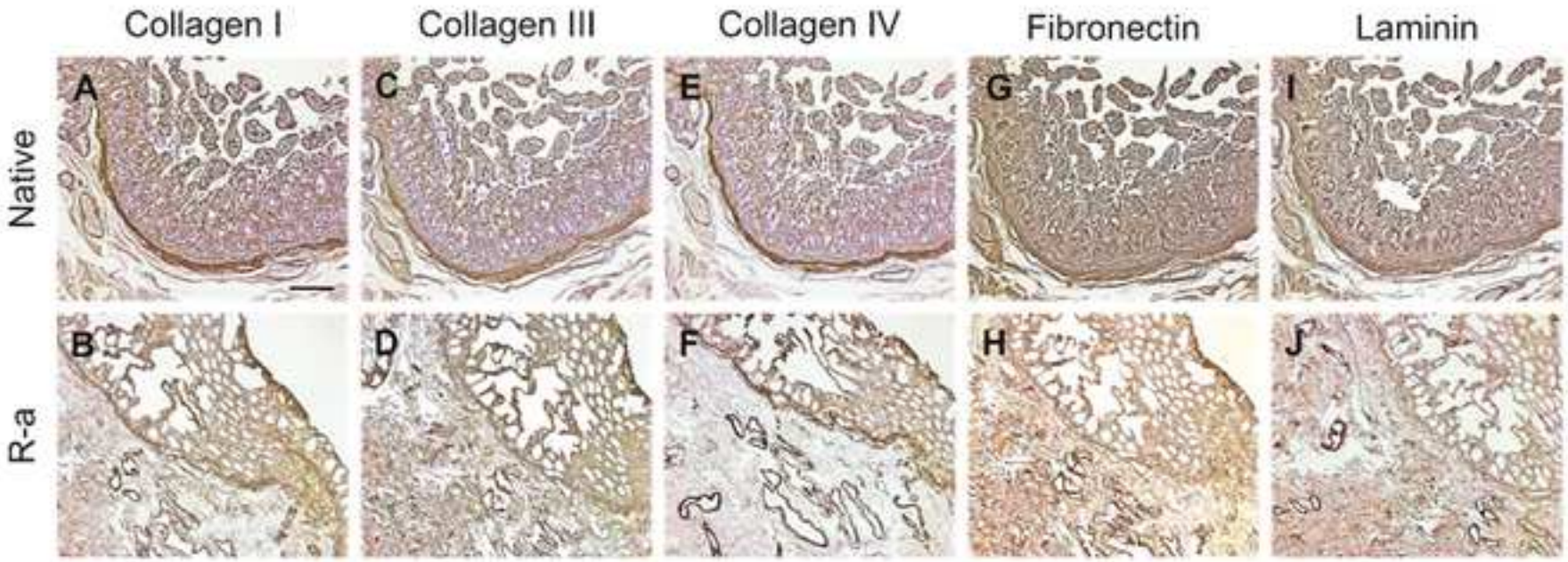


Figure 2

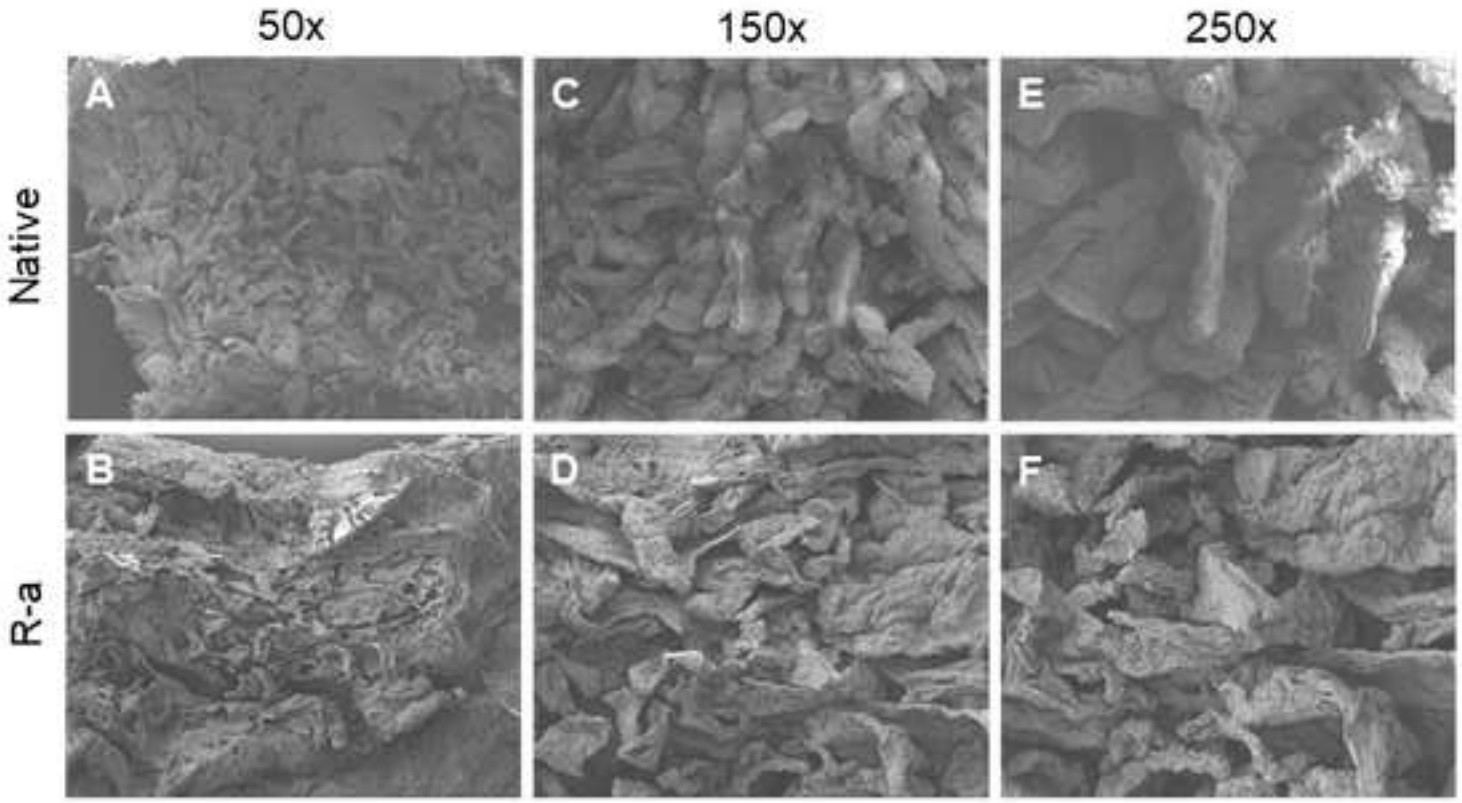


Figure 3

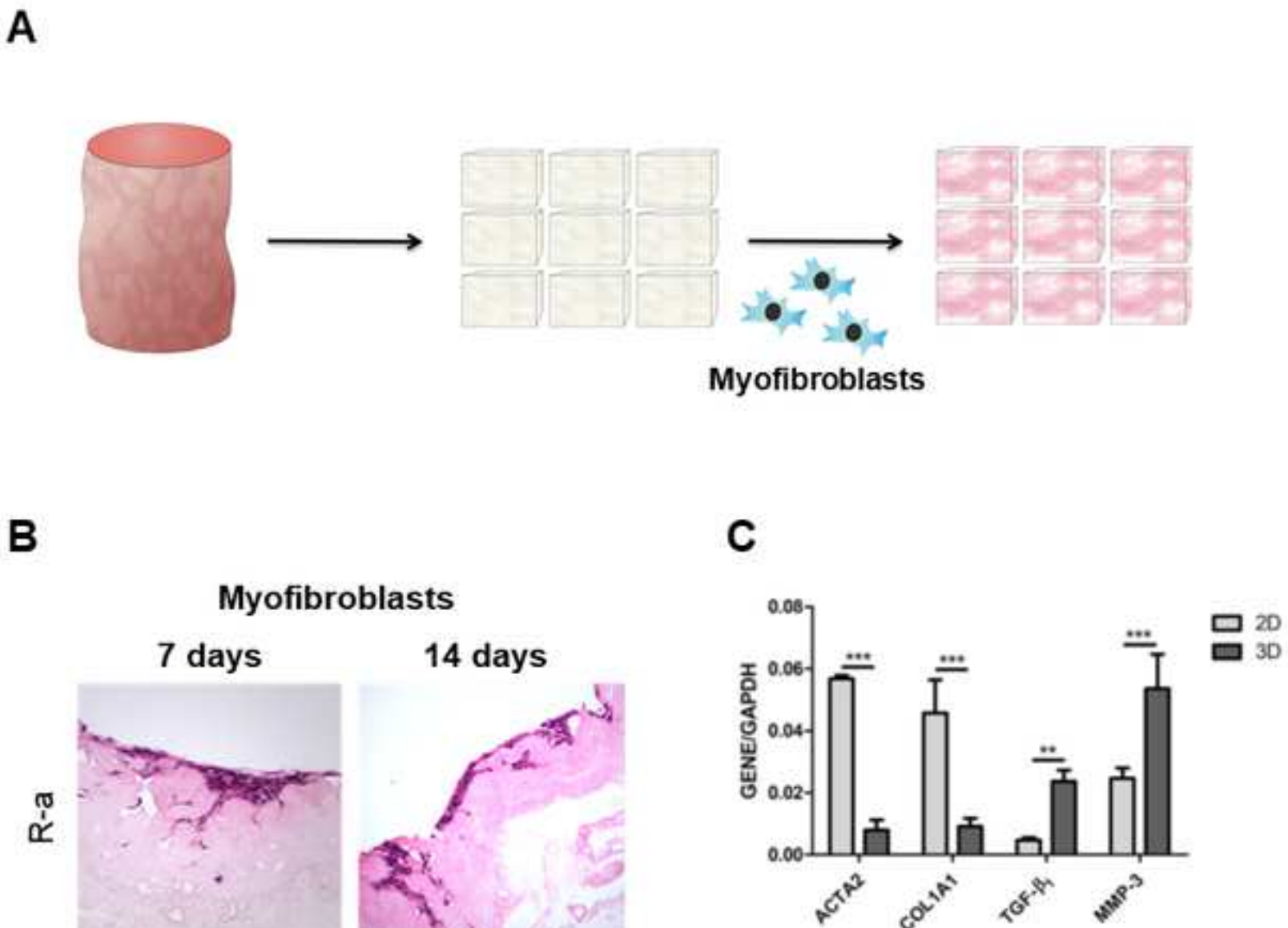


Figure 4

Image

Click here to access/download;Image;Rev Figure 5 21Apr19.tif

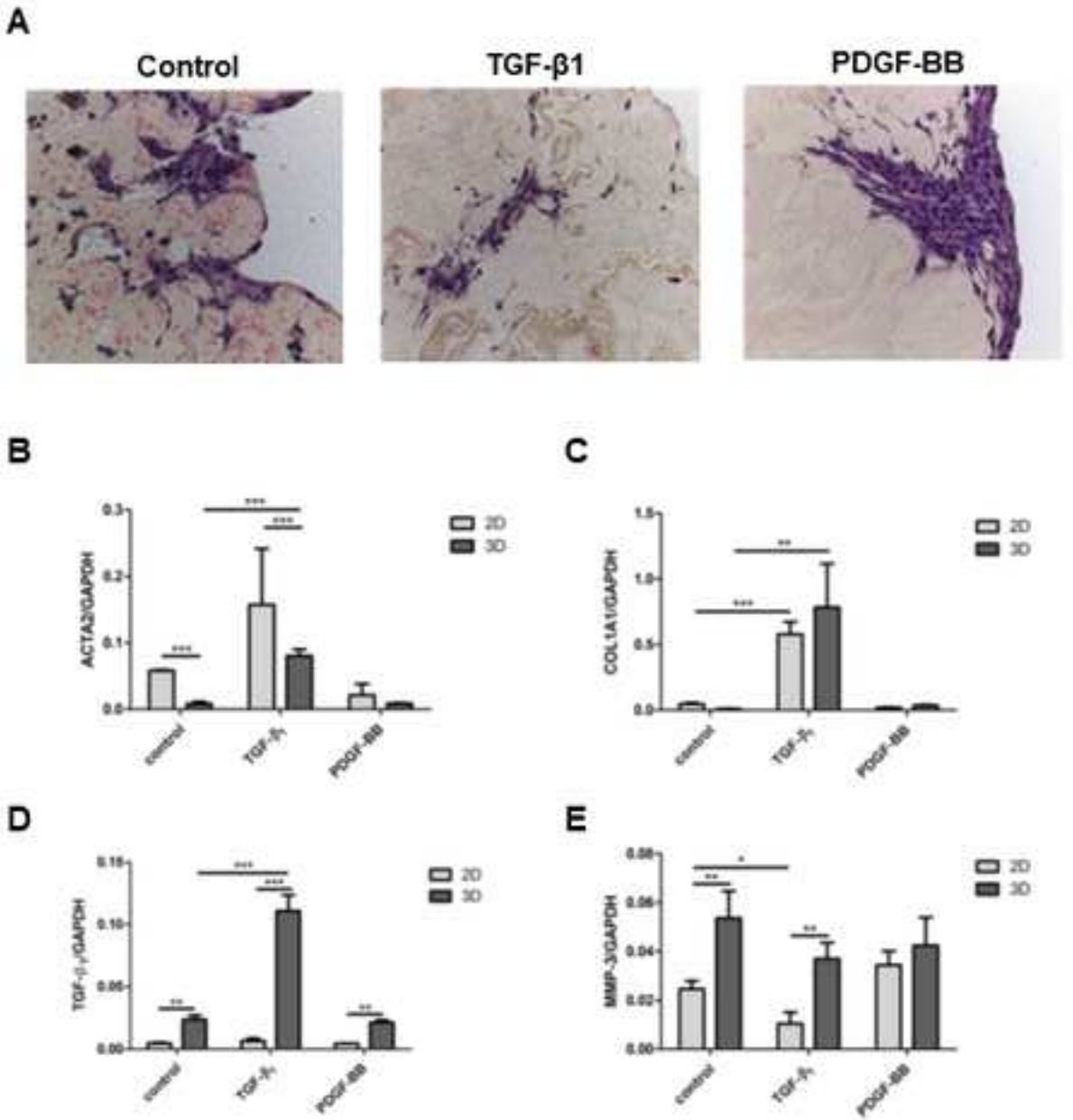


Figure 5